UNIVERSITÀ
DI SIENA
1240

Dipartimento di Biotecnologie Mediche

Dottorato in Biotecnologie Mediche

38° Ciclo

Coordinatore: Prof. Francesco Iannelli

In vitro molecular identification and characterization of investigational and licensed antivirals against viral pathogens

Candidato/a

Niccolò Bartolini

Sede di attività

Department of Medical Biotechnologies, Siena, Italy

Firma digitale del/della candidato/a

Supervisore

Prof. Maurizio Zazzi

Ente di appartenenza

Department of Medical Biotechnologies, Siena, Italy

Co-supervisore/i

Prof. Francesco Saladini

UNIVERSITÀ DI SIENA 1240
Firmato digitalmente da Niccolo Bartolini
Data: 26.03.2026 17:35:50 CET

Ente di appartenenza
Department of Medical Biotechnologies, Siena, Italy

Anno accademico di conseguimento del titolo di Dottore di ricerca
2024/25

Università degli Studi di Siena
Dottorato in Biotecnologie Mediche
38° Ciclo

Data dell'esame finale

_____

Commissione giudicatrice

_____
_____
_____
_____
_____

Supplente

_____

TABLE OF CONTENTS

LIST OF ABBREVIATIONS

2DR	2-drugs regimen
3DR	3-drugs regimen
3TC	Lamivudine
AIDS	Acquired immunodeficiency syndrome
ART	Antiretroviral therapy
ATV	Atazanavir
BIC	Bictegravir
CA	Capsid protein
CAB	Cabotegravir
CAD	Cell-associated DNA
CAR	Cell-associated RNA
CC_{50}	Half-maximal cytotoxic concentration
CCR5	C-C chemokine receptor 5
CI	Capsid inhibitor
CMP	Compound
CRF	Circulating recombinant forms
CXCR4	C-X-C chemokine receptor 4
DENV	Dengue virus
DMEM	Dulbecco's Modified Eagle's Medium
DOR	Doravirine
dPCR	Digital PCR
DRV	Darunavir
DTG	Dolutegravir
EC_{50}	Half-maximal effective concentration
EFV	Efavirenz
FBS	Fetal bovine serum
FC	Fold-change
FDA	Food and Drugs Administration
FI	Fusion inhibitor
FTC	Emtricitabine
FTR	Fostemsavir
HIV	Human immunodeficiency virus
HTE	Heavily-treatment experienced
IBA	Ibalizumab
IC_{50}	Half-maximal inhibitory concentration
IN	Integrase
INSTI	Integrase strand transfer inhibitor
IP	Intact proviruses
IQR	Interquartile range

ISL	Islatravir
IVRS	*In vitro* resistance selection
LEN	Lenacapavir
LTR	Long terminal repeats
MDR	Multidrug-resistant
MHC-II	Major histocompatibility complex class II
MOI	Multiplicity of infection
NNRTI	Non-nucleoside reverse transcriptase inhibitor
NRTI	Nucleoside reverse transcriptase inhibitor
NRTTI	Reverse transcriptase translocation inhibitor
OBR	Optimized background regimen
PBS	Phosphate buffered saline
PI	Protease inhibitor
PIC	Pre-integration complex
PR	Protease
PrEP	Pre-exposure prophylaxis
PS	Penicillin and streptomycin
PWH	People with HIV
RAM	Resistance-associated mutation
RPMI	Roswell Park Memorial Institute
RPV	Rilpivirine
RT	Reverse transcriptase
SARS-CoV-2	Severe acute respiratory syndrome - Coronavirus 2
SC	Subcutaneously injectable
SD	Standard deviation
SI	Selectivity index
SIV	Simian immunodeficiency virus
TAF	Tenofovir alafenamide
TAM	Thymidine analog mutation
TCR	T-cell receptor
TDF	Tenofovir disoproxil fumarate
TN	Treatment-naïve
ZIKV	Zika virus

1 MY PHD ACTIVITIES

During my three years period (2023-2025, 38th cycle) of attendance at the PhD course in Medical Biotechnologies, I was part of the laboratory of Microbiology and Virology at the Department of Medical Biotechnologies of the University of Siena. The PhD course was funded by the European Union Next Generation EU, within the framework of the "Piano Nazionale di Ripresa e Resilienza (PNRR)" program.

Since 1990, the Department has hosted the HIV Monitoring Laboratory (HML), originally established as a public health service and subsequently involved in numerous research projects relating to the Human Immunodeficiency Virus (HIV). In recent years, HML has expanded its research focus on emerging and re-emerging flaviviruses such as Dengue virus, West Nile virus and Zika virus, and more recently, to the newly identified severe acute respiratory syndrome - Coronavirus 2 (SARS-CoV-2), responsible of the recent pandemic. Viruses have been recognized as major causative agents for a wide spectrum of diseases in humans, from mild and self-limiting infections to severe and potentially fatal outcomes. Generally, most of the viral diseases are divided into either acute or chronic. Acute viral infections arise characteristically with a sudden onset of symptoms, which vary from mild to severe, and a resolution period, limited to few days, which can end without sequelae or even with death. On the other hand, chronic viral infections persist in target host cells by mechanisms such as latency, continuous replication or silent and productive turnover periods, putting serious risks the host health (Deigendesch and Stenzel, 2018). The current strategy for fighting viral diseases relies on large-scale vaccination programs combined with the administration of antiviral drugs. However, only a limited number of viral pathogens have effective vaccines, leading to an increasing demand for new antiviral strategies. This need is driven by the rise in chronic viral infections, the emergence of new and highly transmissible viruses, and the re-emergence of previously controlled pathogens. Moreover, viruses that were once geographically restricted are now spreading and becoming established in new regions mostly because of globalization and climate change. (Pierson and Diamond, 2020). Despite recent rapid advancements in *de novo* drug design that have significantly accelerated early-stage drug discovery, the pathway to approval of new therapeutics remains long and economically burdensome. Consequently, drug repurposing has become a more attractive

alternative, providing a cost-effective and time-efficient strategy for identifying safe antiviral candidates. Irrespective of whether candidate molecules are novel or repurposed, *in vitro* assessment of antiviral activity remains the most critical step in the screening process. Among the available methodologies, cell-based assays represent one of the most powerful tools for assessing antiviral efficacy (Boldescu *et al.*, 2017; García-Serradilla, Risco and Pacheco, 2019).

During my PhD, I had the opportunity to work on different topics, collaborating with many brilliant scientists and institutions who broaden my horizons, increasing my expertise on many applications and techniques.

1.1 Evaluation of broad-spectrum piperazine-based compounds able to inhibit flavivirus and/or SARS-CoV-2 replication in a live virus assay

In collaboration with the Department of Organic and Medicinal Chemistry of the University of Seville, I was involved in the identification and characterization of novel antiviral compounds targeting emerging and re-emerging viral pathogens of major public health relevance. This work has focused on three viruses for which therapeutic options remain limited: Zika virus (ZIKV), Dengue virus (DENV), for which no specific antiviral drugs are currently available, and SARS-CoV-2, against which only three approved antivirals are currently in clinical use, namely, Remdesivir, Molnupiravir and Nirmatrelvir, with this latter particularly indicated for treatment of people at high risk of hospitalization (WHO, 2025). The central aim of my research was to evaluate the *in vitro* antiviral activity of a panel of newly synthesized small molecules (CMPs) against these pathogens and to investigate their potential as candidates for further antiviral development. These molecules were designed by means of a privileged structure-based approach based on a piperazine scaffold. Accordingly, two main families were developed: the first carrying a 2-phenyl piperazine core (compounds 1-29) and the second based on an unsubstituted piperazine-backbone (compounds 30-51).

The first step was to determine the cytotoxicity profile (half-maximal cytotoxic concentration, CC_{50}) for all compounds in two human cell lines competent for viral infection: A549 ACE2-TMPRSS2 (A549-AT) for SARS-CoV-2 and Huh7 hepatoma cells for ZIKV and DENV. Only non-toxic concentrations were used for antiviral assays. Further, cells were treated with the selected CMPs

and infected with a multiplicity of infection (MOI) of 0.001 with the corresponding virus. Antiviral activity was quantified by immunodetection of viral proteins: nucleocapsid for SARS-CoV-2 and envelope protein for ZIKV and DENV. From these data, half-maximal inhibitory concentration (IC_{50}) and selectivity index (SI) were calculated, in order to compare efficacy and cytotoxicity. All statistical analysis were performed using GraphPad Prism software (v 9.0.0).

Results (**Table 1**) highlighted several candidates with promising profiles. Within the first family of compounds, median (IQR) CC_{50} values were 62 µM (22.7 - 200.0) in Huh7 cells and 138 µM (36.5 - 200) in A549-AT cells, whereas compounds from the second family were generally associated with a reduced cytotoxicity (400 µM [112.9 - 400.0] and 130 µM [89.4 – 400.0], in Huh7 and A549-AT, respectively). Of all the molecules tested, CMPs 24 and 26 showed selective activity against ZIKV within the low micromolar range (IC_{50} 2.5±1.4 and 9.6±4 µM, respectively). More interestingly, CMP 50 was identified as a broad-spectrum molecule capable of inhibiting both ZIKV and SARS-CoV-2, with a particularly favorable SI for ZIKV (148.1). In addition, nine compounds exhibited anti-ZIKV activity below 15 µM and four of them (CMPs 35, 39, 41, and 42) showed inhibition also against DENV (67.9±5.4 µM, 33.8±3.3 µM and 11.7±2.2 µM, respectively). Compounds with IC_{50}<15 µM were further studied by enzymatic assays and molecular docking to fully describe the interaction with the viral enzyme active site, supporting structural optimization. Among the most promising molecules, CMP 50 had stronger anti-ZIKV activity (2.7±0.7 µM) than Sofosbuvir (3.7±0.9 µM), although it remained less potent against SARS-CoV-2 than Nirmatrelvir (22.5±1.5 µM vs. 0.04±0.0 µM). Importantly, the relatively low structural complexity makes CMP 50 an excellent candidate for future structure-guided improvement. In addition, CMPs 41, 42, and 49 gave potent inhibitions of ZIKV with IC_{50} values below 5 µM (4.6±0.7 µM, 1.6±0.0 µM and 3.2±0.9 µM, respectively). CMP 42 exhibited a higher SI (250) compared not only to Sofosbuvir but also to other compounds in the panel. Taking altogether, these results suggested that piperazine-based molecules are a promising starting point for the development of next-generation antiviral agents. Their activity against ZIKV and DENV make such compounds good candidates for the development of broad-spectrum therapeutics targeting flaviviruses, for which effective treatments are still urgently needed.

These findings were presented at ICAR (Italian Conference on AIDS and Antiviral Research, poster n° 97) 2024, SIV-ISV (Società Italiana di Virologia – Italian Society for Virology, poster n° 045) conference 2024 and at SIM (Società Italiana di Microbiologia, poster ° 045) conference 2024.

		CC_{50} µM		IC_{50} µM			SI		
Compound	**Family**	**Huh7**	**A549-AT**	**ZIKV Huh7**	**DENV Huh7**	**SARS-CoV-2 A549-AT**	**ZIKV**	**DENV**	**SARS-CoV-2 WT**
24	**1°**	200,0	400,0	2,5 ± 1,4	NT	NT	80,0	NT	NT
26	**1°**	24,0	22,0	9,6 ± 4,0	NT	NT	2,5	NT	NT
34	**2°**	400,0	109,0	27,9 ± 5,3	NA	NA	14,3	NT	NT
35	**2°**	182,0	95,4	48,1 ± 0,3	67,9 ± 5,4	NA	3,8	2,7	NT
37	**2°**	400,0	200,0	38,7 ± 0,7	NA	NA	10,3	NT	NT
38	**2°**	53,0	21,0	5,1 ± 0,0	NA	NA	10,4	NT	NT
39	**2°**	155,7	84,0	13,2 ± 0,4	33,8 ± 3,3	NA	11,8	4,6	NT
41	**2°**	400,0	188,0	4,6 ± 0,7	11,7 ± 2,2	NA	87,5	34,3	NT
42	**2°**	400,0	28,6	1,6 ± 0,0	3,8 ± 0,7	NA	250,0	105,5	NT
43	**2°**	400,0	400,0	159,0 ± 48,3	NA	NA	2,5	NT	NT
44	**2°**	400,0	400,0	43,7 ± 3,6	NA	NA	9,2	NT	NT
49	**2°**	400,0	151,1	3,2 ± 0,9	NA	NA	127,0	NT	NT
50	**2°**	400,0	169,9	2,7 ± 0,7	NA	22,5 ± 1,5	148,1	NT	7,6
NRM	**/**	NT	40,0	NT	NT	0,04 ± 0,0	148,1	NT	1000,0
SOF	**/**	400,0	NT	3,7 ± 0,9	4,3 ± 1,4	NT	108,0	93,0	NT

***Table 1**: antiviral activity and cytotoxicity of first and second family compounds against ZIKV, DENV and SARS-CoV-2. CC_{50} = half-maximal cytotoxicity concentration; IC_{50} = half-maximal inhibitory concentration; NT = not tested; NA = not active; NRM = Nirmatrelvir; SOF = Sofosbuvir*

1.2 Proteomic investigation of human molecular targets modulated by pyridobenzothiazolone-derivative compound as an antiviral treatment against West Nile Virus

Another line of research pursued during my PhD focused on the understanding of the antiviral mechanism of a promising class of compounds active against flaviviruses including DENV, ZIKV and West Nile virus (WNV). As noted previously, these viruses have emerged or are currently emerging in regions where they were not previously present, posing significant new public health challenges. Although most infections remain asymptomatic, a subset of individuals develop severe and sometimes life-threatening diseases.

Within this context, recent studies have identified pyridobenzothiazolone (PBTZ) derivatives as potent antiviral agents. The compound HeE1-17Y (17Y) is of particular interest since it has demonstrated broad-spectrum activity across several flaviviruses, including multiple DENV serotypes and ZIKV. Although a previous work suggested that 17Y exerts both virucidal activity, directly disrupting viral particles, and potential inhibition of the highly conserved NS5 RNA-dependent RNA polymerase (Milan Bonotto *et al.*, 2022), very little was known about how 17Y interacts with host cell pathways both in the presence and absence of viral infection.

To investigate these characteristics, the Functional Proteomics Lab of the Department of Life Sciences of the University of Siena, performed a differential proteomic analysis consisting in 2-dimensional electrophoresis (2DE) and liquid chromatography-tandem mass spectrometry (LC-MS/MS) using human Huh7 cells infected with WNV at a MOI of 0.005. Two experimental conditions were tested: addition of 17Y during the infection to investigate virucidal effects, and post-infection addition to assess its impact on later stages of the viral life cycle. This approach allowed deeper to define potential differences in cellular responses depending on the timing of drug interaction with the infected system.

Experimental results indicated that 17Y altered the expression of several host proteins in uninfected cells, including the ATP-dependent RNA helicase DDX3X and the mitochondrial inner membrane protein MIC60, both of which could be involved in viral replication processes. In infected cells, 17Y consistently reduced the abundance of viral NS3 and NS1 non-structural proteins under both treatment protocols, suggesting its possible role in limiting the generation of new viral particles. Only minimal differences between the two infection-treatment conditions were observed; however, two main pathways were detected by enrichment analyses: i) a significant dysregulation of the Krebs cycle, as reflected by down-regulation of the key enzymes aconitase (ACON), fumarate hydratase (FUMH), pyruvate carboxylase (PYC) and succinate dehydrogenase subunit A (SDHA); (ii) changes in the host-virus interaction processes supported by dysregulation of the ALG-2 Interacting Protein X (ALIX) and the small ribosomal subunit protein uS2/RPSA.

Globally, these findings help further elucidate the mechanism of action of 17Y in antiviral activity and possible off-target influences at the cellular level, supporting further development of compounds derived from PBTZ as candidates for broad-spectrum anti-flavivirus therapy.

This work was performed in the context of the INF-ACT network and in collaboration with the “Istituto di Biofisica - Consiglio Nazionale delle Ricerche (IBF-CNR)”, Research Node (RN) 5, the University of Siena (RN 1 and 5), and the University of Perugia, thanks to the PANVIRIDAE (Preparedness Against Newly-emerging Viruses: Innovations in Research, Intervention, and Drug Evolution) project. This collaboration was made possible with the support of the Italian Ministry of Education, University and Research (MUR) under the PNRR-PE13 INF-ACT program, which focuses on One Health-oriented research related to emerging infectious diseases.

1.3 Combined doravirine and islatravir cooperate to inhibit NRTI and NNRTI resistant HIV-1 *in vitro*

Clinical management of multidrug-resistant (MDR) HIV-1, particularly in heavily-treatment experienced (HTE) people with HIV (PWH), is still hard challenging. While doravirine, a non-nucleoside reverse transcriptase inhibitor (NNRTI), has been approved for both initiation and switch/maintenance therapy based on its favorable resistance profile and high genetic barrier to resistance, islatravir, a first-in-class nucleoside reverse transcriptase translocation inhibitor (NRTTI), represents an investigational agent with a unique mechanism of action that can inhibit viral reverse transcriptase translocation. This may offer potential activity against viruses resistant to conventional NRTIs. Recent *in vitro* studies supported the hypothesis that the combination of doravirine and islatravir may delay the emergence of resistance mutations and provide synergistic or additive antiviral effects (Brenner *et al.*, 2023). However, the comprehensive evaluation in clinically derived multidrug-resistant isolates had not been performed yet.

Therefore, during my PhD I contributed to a research project that aimed to assess the *in vitro* activity of doravirine and islatravir, alone and in combination, against HIV-1 isolates harboring complex resistance mutation patterns to NRTIs and NNRTIs.

The sample dataset included 39 recombinant viruses derived from plasma of 38 HTE PWH enrolled in the Italian PRESTIGIO registry (https://registroprestigio.org/), which includes PWH with 4-drug-class-resistant HIV defined as an intermediate or high resistance to ≥1 NRTI, ≥1 NNRTI, ≥1 PI, and ≥1 INSTI according to the Stanford algorithm (version 9.5, https://hivdb.stanford.edu/). Recombinant viruses were prepared by homologous recombination using a modified NL4-3 backbone and *in vitro* susceptibility was measured using a TZM-bl-based assay, calculating fold-change (FC) values relative to the IC_{50} of the wild-type NL4-3 reference strain. All statistical analysis were performed using GraphPad Prism software (v 9.0.0).

In the phenotypic analyses, doravirine demonstrated full susceptibility in 15/39 (38.5%) viruses, while 9/39 (23.1%) showed high-level resistance as defined by an FC value above 100. The viruses carrying doravirine resistance-associated mutations (n = 13) had a significantly higher median (IQR) FC of 100 (16.4 - 100) compared to those without mutations at 2.4 (0.6 - 6.6) ($p < 0.0001$,

Kruskal-Wallis test). Of interest, four isolates demonstrated enhanced susceptibility to doravirine (FC < 0.4), including two from the same PWH with E138A+G190A and two others with either K103N+Y181I or K101E+E138K, indicating that certain combinations of NNRTI mutations may enhance susceptibility.

The global median (IQR) FC value for islatravir was 3.9 (1.3 - 10.4), while the median (IQR) FC for viruses harboring the M184V/I mutation (n = 26) was considerably higher than for those without the mutation (7.7 [3.6 - 13.2] vs. 1.3 [0.8 - 2.2], $p < 0.0001$, Kruskal-Wallis test), confirming the negative impact on the susceptibility. The total number of NRTI resistance mutations and the number of thymidine analog mutations (TAMs) positively correlated with islatravir FC (Rho = 0.342, p = 0.03; Rho = 0.597, respectively, $p < 0.001$, Spearman's correlation), with greater numbers of TAMs leading to increased resistance even among the subset of viruses bearing M184V/I. However, some exceptions have been identified, with one virus harboring only M184V that caused an FC value of 10.4, while two isolates showed increased islatravir susceptibility, including one virus with a mixed L74LI pattern and another with complex NRTI mutation patterns including A62V, D67N, K70E, V75I, Y115F, F116Y, Q151M, and M184V. These findings indicated that the viral genetic background and specific mutation combinations have the potential to modulate islatravir susceptibility.

Both the SynergyFinder Plus (https://synergyfinder.org/and) and the Multi-dimensional Synergy of Combinations (MuSyC, https://musyc.lolab.xyz/) tools were used to analyze the combinatorial activity of doravirine and islatravir. The ZIP model of SynergyFinder Plus revealed additive activity in 37/40 cases (92.5%), synergistic activity in one case, demonstrating enhanced doravirine susceptibility and antagonistic activity in two cases (both resistant to doravirine but fully susceptible to islatravir). Combination Sensitivity Scores (CSS) were higher than wild-type NL4-3 in 22/39 (56%) viruses, indicating that resistance mutations may not impair the combinatorial efficacy. Analysis with the MuSyC model showed that 25/40 (62.5%) viruses, including the wild-type, displayed synergistic interactions, according to values of the β parameter > 0. The β parameter negatively correlated with doravirine FC (Rho = -0.409, p = 0.009), number of NRTI mutations (Rho = -0.328, p = 0.039) and presence of M184V/I (Rho = -0.377, p = 0.018), indicating that high-level doravirine resistance and extensive NRTI mutational patterns decrease the cooperative effect of the drug combination. Notably, islatravir FC did not correlate with the β parameter, suggesting that doravirine susceptibility may be the main driver of combinatorial

efficacy. Directional synergistic effects were further underlined by the α parameter, showing that high dose islatravir synergized with doravirine IC_{50} in 24/37 cases (64.9%), whereas doravirine synergizes with islatravir IC_{50} in 19/40 cases (47.5%). Confirmed synergy and antagonism based on both α1→2 and α2→1 was found in 16 (40%) and 11 (27.5%) cases, respectively. Indeed, α2→1 also negatively correlated with the number of NRTI mutations (Rho = -0.377, p = 0.016), confirming that cooperative activity is reduced upon accumulation of NRTI resistance. In summary, these data suggest that doravirine and islatravir retain significant activity against multidrug-resistant HIV-1 isolates, and the combination of these agents is effective at inhibiting viral replication in the presence of complex resistance profiles. This study emphasizes the potential utility of this drug combination for use in salvage therapy among HTE PWH and underlines the importance of integrating phenotypic susceptibility testing with combinatorial analyses in informing appropriate treatment decisions.

The results of this study were described in a manuscript published as research article in the Antiviral Research journal (see **chapter 7**).

1.4 Comparative analysis of islatravir and tenofovir alafenamide *in vitro* activity in NRTI-resistant HIV-1 harbouring the M184V/I mutation

As stated in the previous paragraph, multidrug resistance remains one of the major challenges in sustaining long-term antiretroviral efficacy. Mutations associated with resistance to nucleoside reverse transcriptase inhibitors (NRTIs) can greatly impair treatment responses, directly limiting the therapeutic options available for PWH experiencing virological failure. In this context, evaluating the residual activity of molecules within the drug class, or of candidate molecules belonging to closely related classes, may be essential for identifying drugs that retain activity and may be incorporated in salvage therapies. Based on these considerations, I was involved in the investigation of the antiviral susceptibility of multidrug-resistant HIV-1 strains, focusing on the impact of the M184V/I resistance mutation on NRTI therapy. This resistance mutation is well-known to strongly decrease the activity of both lamivudine and emtricitabine, while modestly increasing susceptibility to tenofovir (Turner, Brenner and Wainberg, 2003). Previous *in vitro*

studies also suggested that M184V/I may decrease susceptibility to the first-in-class NRTTI, islatravir (ISL), when combined with other NRTI resistance-associated mutations (Kawamoto *et al.*, 2008). The study I was involved aimed to directly compare the *in vitro* antiviral activity of ISL, currently under clinical evaluation for the treatment of multidrug-resistant HIV-1 infections, and the NRTI tenofovir alafenamide (TAF), against clinically derived HIV-1 isolates harboring the M184V/I mutation and multiple additional NRTI mutations. First, recombinant viruses carrying clinically derived protease and reverse transcriptase (PR-RT) sequences from 23 HTE PWH enrolled in the Italian PRESTIGIO registry. All isolates carried multiple NRTI resistance mutations, including M184V/I, and most also harbored NNRTI mutations. *In vitro* susceptibility was measured using a TZM-bl-based assay, calculating FC values relative to the IC_{50} of the wild-type NL4-3 reference strain. All statistical analysis were performed using GraphPad Prism software (v 9.0.0). Genotypic and phenotypic susceptibility to TAF was also evaluated and compared using the Stanford HIVdb algorithm (v9.5.1) and established Monogram phenotypic clinical cut-off values (lower/upper cut-off 1.4/4.0).

The median (IQR) IC_{50} FC value was 7.3 (3.9 - 13.0) for ISL and 2.7 (1.3 - 4.5) for TAF ($p < 0.0001$, Wilcoxon signed rank test) (**Figure 1**), reflecting generally higher resistance to ISL among these isolates. Whereas the degree of resistance to ISL was unrelated to the total number of Thymidine Analog Mutations (TAMs) and NRTI mutations, specific mutational patterns including M184I together with nine additional NRTI mutations resulted in the highest FC (37.8) observed for ISL. The NNRTI resistance mutation V106I coupled with M184V was found in a virus showing one of the highest ISL FC values, confirming a possible cooperation of these two mutations in reducing ISL susceptibility (Aulicino *et al.*, 2024). Statistical analyses indicated that K65R mutation was associated with the highest TAF FC values (7.7 and 4.9), whereas in the absence of K65R, TAF resistance was positively correlated with the total number of NRTI and TAMs ($p = 0.012$ and $p = 0.002$, respectively, Spearman's rank test). Genotypic predictions of TAF susceptibility were mostly concordant with phenotype results, although some discrepancies were noted. Overall, results suggested that HTE PWH-derived viruses harboring M184V/I may take advantage more from TAF- than from ISL-based regimen. These findings also demonstrate the need for phenotypic testing to guide treatment decisions in the context of complex resistance mutational patterns.

In summary, this study could contribute significantly to a better understanding of how specific resistance mutations affect the activity of new and established NRTIs and could provide critical insight into therapy optimization strategies for multidrug-resistant PWH management.

These data were presented at EMHH (European Meeting on HIV and Hepatitis, poster n° 53) 2024 and ICAR 2024 (Short Communication).

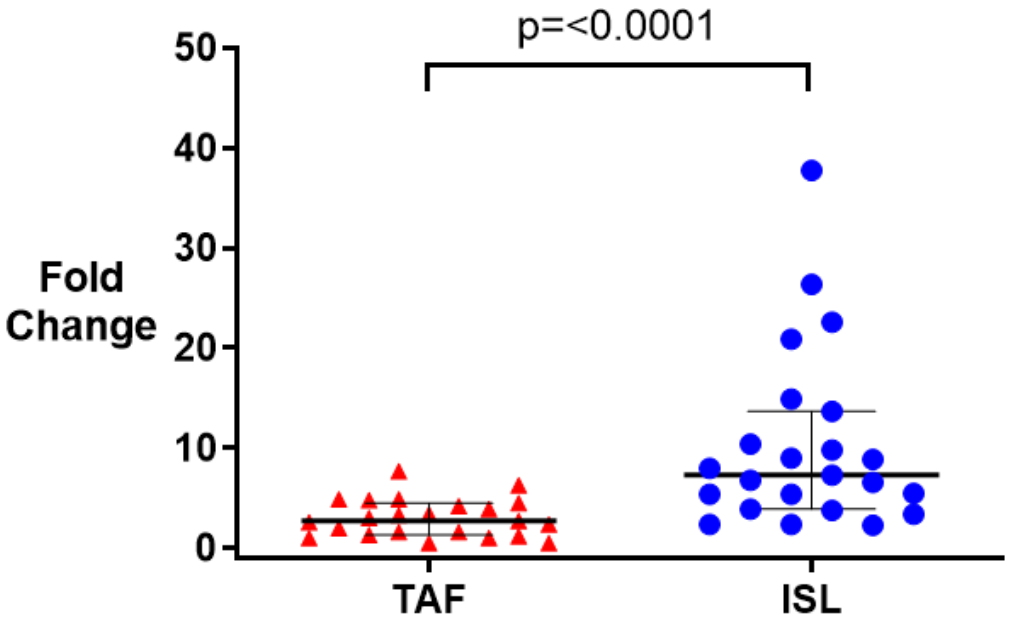

***Figure 1**: comparison of fold-change Tenofovir alafenamide (TAF) and Islatravir (ISL) susceptibility*

1.5 Comparable dynamics of cell-associated HIV-RNA, total and intact proviral HIV-1 DNA in virologically suppressed people with HIV switching to 2DR or continuing 3DR over an 18-month follow-up

During my PhD, I took part in a project named MARISA (Multidisciplinary Assessment of the HIV Reservoir and Immunity following Switch from 3-drug to 2-drug Antiretroviral Regimens in virologically suppressed patients), which was funded through the PRIN (Progetti di Ricerca di Rilevante Interesse Nazionale) initiative of the Italian Ministry of University and Research. The University of Siena was involved in the project investigating whether simplification of antiretroviral therapy could affect cell-associated HIV molecular markers (HIV-RNA, HIV-DNA and intact proviruses) in $CD4^+$ T cells. Understanding how the viral reservoir responds to treatment

modifications is critical for informing therapy simplification strategies and long-term management approaches.

Briefly, a total of 67 virologically suppressed PWH, 32 of whom remained on 3DR and 35 who were switched to 2DR, were enrolled in this observational study. Assessments were made upon enrollment (T0) and 18 months after enrollment (T1). Cell-associated HIV-RNA (CAR) was measured using a digital PCR (dPCR) assay targeting LTR, while HIV-DNA (CAD) and intact proviruses (IP) were quantified by a triplex dPCR targeting LTR for CAD and psi and ENV regions for IP. All dPCR assays were run on a QIAcuity (Qiagen) platform. All statistical analyses were performed using IBM SPSS Statistics 20 software.

At T0, participants had a median (IQR) age of 45 years (12), and 97% were male. Nadir and baseline $CD4^+$ counts were 388 (281) and 795 (399) cells/μL, respectively, while zenith HIV-1 RNA was 4.9 (1.1) log copies/mL. and time under therapy was 54.5 (61.8) months. The 2DR and 3DR groups were comparable in most parameters except for age (41 [11] vs. 49 [14], p = 0.008, Mann-Whitney test) and nadir $CD4^+$ cells count (437 [275] vs. 291 [369], p = 0.007, Mann-Whitney test). Baseline CAD and CAR were 2.7 (1.2) and 3.8 (1.3) log copies per million $CD4^+$ T-cells, respectively, while IP was 4% (14%), with no significant differences between treatment groups. Notably, 11 out of 67 (16.4%) IP samples failed amplification at one or both targets. At T0, CAD inversely correlated with nadir $CD4^+$ (Rho = -0.304, p = 0.012, Spearman's rank correlation, **Figure 2A**) and positively correlated with CAR (Rho = 0.653, p < 0.001, Spearman's rank correlation, **Figure 2B**), while CAR also inversely correlated with nadir CD4+ (Rho = -0.411, p = 0.001, Spearman's rank correlation, **Figure 2C**).

Over 18 months, the overall reservoir markers remained stable, having only few median changes in CAD (+0.19 log), CAR (-0.1 log), and IP (0%). Of note, IP decreased more in the 2DR group when compared to the 3DR group (-6.5% vs. +0.5%, p = 0.036, Spearman's rank correlation), supporting a slight but quantifiable effect of treatment simplification on intact proviruses. This finding was complemented by regression analyses showing that higher baseline CAD values were associated with smaller changes over time (B = 0.499, p < 0.001) consistent with a plateau effect, whereas baseline IP and CAD levels follow only a negative trend.

These findings indicate that switching from 3DR to 2DR does not significantly alter surrogate markers of the HIV reservoir over a period of 18 months. Importantly, this study underlines the

relative stability of CAR, CAD, and IP, with further research required into the clinical implications of intact provirus measures in both HIV reservoir dynamics and therapy simplification.

These data were presented at ICAR 2025 (Short Communication), EMHH 2025 (Oral Presentation), EU2Cure HIV Symposium 2025 (Poster n°25) and at EACS (European AIDS Clinical Society, poster n° eP055).

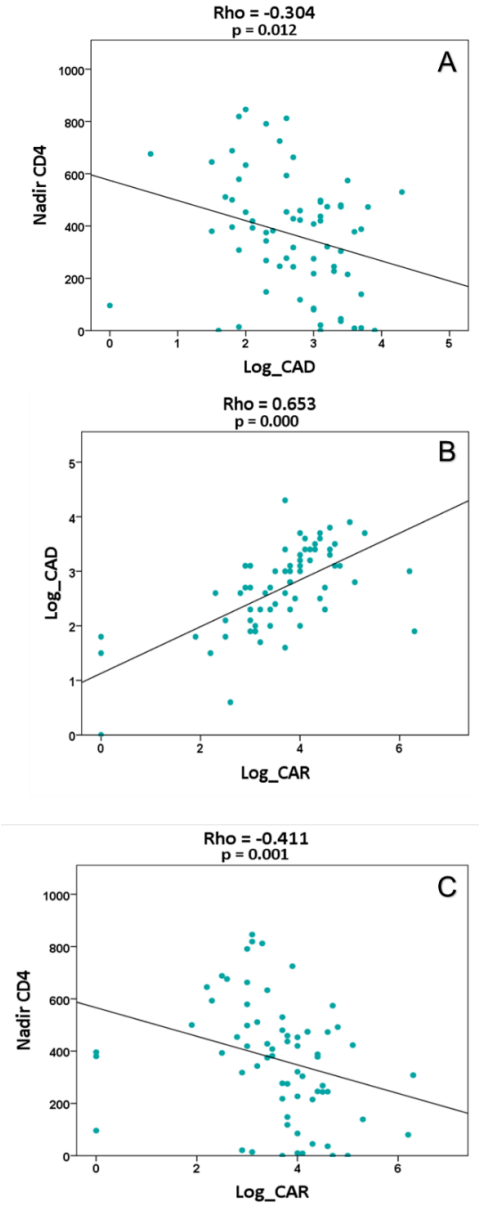

***Figure 2**: significative Spearman's correlations between* baseline *CAD* and nadir $CD4^+$ (A); baseline CAD and baseline CAR (B); baseline CAR and nadir $CD4^+$. CAD = cell-associated DNA; CAR = cell-associated RNA

2 INTRODUCTION

2.1 HIV background

The Human Immunodeficiency Virus (HIV) is a Lentivirus belonging to the *Retroviridae* family and it is the etiological agent of the acquired immunodeficiency syndrome (AIDS) (Gallo *et al.*, 1984; Popovic *et al.*, 1984). First isolated in 1983 by two different research groups (Barré-Sinoussi *et al.*, 1983; Gallo *et al.*, 1983), it was further characterized into HIV-1 and HIV-2 strains by serological and immunological comparison. HIV-2 was discovered in 1986 in West Africa, where it still remains endemic, in patients with AIDS symptoms, but negative to HIV-1 antibodies (Clavel *et al.*, 1986). Genetically, HIV-2 appeared to be closely related to the simian immunodeficiency virus (SIV), identified in a group of non-human primates (*Macaca mulatta*) that presented an AIDS-like syndrome (Guyader *et al.*, 1987). Similar simian HIV-1 and HIV-2 were also found in chimpanzees and sooty mangabeys, suggesting that lentiviral cross-infections and zoonosis between humans and primates led to HIV formation (Sharp and Hahn, 2011). Phylogenetically, HIV-1 comprises four different groups, M, N, O and P, with the M group being the main responsible for infections worldwide. This group includes ten distinct subtypes or clades (designated A through L), some of which, such as subtypes A and F, are further divided into sub-subtypes according to their genetic characteristics. Subtypes A, B and C are the most prevalent worldwide, with group C being responsible for nearly 50% of infections (Nair et al., 2024, Buonaguro et al., 2007). According to the most recent UNAIDS HIV update (July 2025), it has been estimated that 40.8 million people globally were living with HIV in 2024, with 1.3 million newly infected. Despite the large and ready access to an efficient antiretroviral therapy (ART), which was administered to 31.6 million patients in 2024 (almost 77% of total infected), 630,000 people died of AIDS-related illnesses (*Fact sheets - UNAIDS*, 2025) (**Figure 3**).

	People living with HIV	People acquiring HIV	People dying from HIV-related causes
Total	**40.8 million** [37.0–45.6 million]	**1.3 million** [1.0–1.7 million]	**630 000** [490 000–820 000]
Adults (15+ years)	**39.4 million** [35.7–44.0 million]	**1.2 million** [950 000–1.5 million]	**550 000** [430 000–720 000]
Women (15+ years)	21.0 million [19.0–23.5 million]	530 000 [410 000–710 000]	240 000 [180 000–320 000]
Men (15+ years)	18.5 million [16.5–20.7 million]	650 000 [530 000–830 000]	320 000 [240 000–410 000]
Children (<15 years)	**1.4 million** [1.1–1.8 million]	**120 000** [82 000–170 000]	**75 000** [53 000–110 000]

***Figure 3**: updated data on the ongoing HIV-1 pandemic, July 2025, WHO/UNAIDS estimation*

Since 2010, there has been a 40% decline in the number of new infections, while HIV-related deaths decreased by 54% (*HIV information sheet - WHO*, 2025). This comes as the direct result of the UNAIDS 95-95-95 program, which aims to diagnose at least 95% of all infected people, to administer ART to at least 95% of those people and to reach virological suppression in at least 95% of people with HIV (*95-95-95 targets - UNAIDS*, 2025) (**Figure 4**).

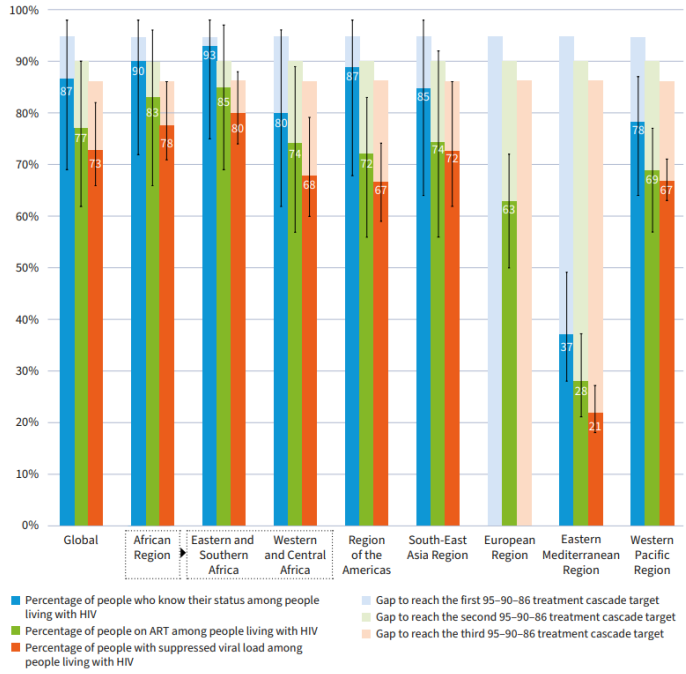

***Figure 4**: 95-95-95 target status, July 2025, WHO/UNAIDS estimation*

2.2 HIV-1 genome organization and morphology

The HIV-1 virion has an icosahedral structure including approximately 14 spikes formed by two different glycoproteins, gp120 and gp41. The outer layer of the HIV-1 virion is derived from the host cell plasma membrane during viral budding and encloses an inner capsid or core, which surrounds two copies of approximately 9.7 kb single-stranded, positive-sense RNA. The RNA genome is associated with nucleocapsid proteins p6 and p7 that protect the viral nucleic. Moreover, three essential enzymes such as viral protease, reverse transcriptase and integrase are present, together with accessory proteins such as Nef, Vif and Vpr (Turner & Summers, 1999). The HIV genome is organized in nine main open reading frames (ORFs) and some overlapping genes that allow to encode for several proteins within a compact genome. At both the 5' and 3' ends, the genome is flanked by non-coding regions divided into the U3, R, and U5 domains, collectively known as long terminal repeats (LTRs). These regions contain information related to integration, gene expression, transcription, and structural regulation. The U5 element is followed by the 18 nucleotide Primer Binding Site (PBS), which is complementary to the cellular $tRNA^{Lys}$ and primes reverse transcription (Mbondji-Wonje et al., 2020). The structural genes *gag*, *pol* and *env* encode major viral proteins. The *gag* gene encodes the $Pr55^{Gag}$ polyprotein, which is cleaved into matrix (p17, MA), capsid (p24, CA), nucleocapsid (p7, NC), and three smaller proteins (p1, p2 and p6) during virion maturation. The *pol* gene encodes the viral protease (p11, PR), reverse transcriptase (p66/p51, RT) and integrase (p31, IN), from the polyprotein precursor $Pr160^{GagPol}$ (Freed, 2002). The regulatory *tat* and *rev* and accessory *vif*, *vpr* and *vpu* genes encode for viral proteins which modulate viral transcription and replication, cellular interaction and immune evasion. The *env* gene encodes two envelope proteins: the surface (gp120, SU) and the transmembrane (gp41, TM) envelope proteins, cleaved by furin-like cellular protease from the gp160 polyprotein (Ramdas *et al.*, 2020) (**Figure 5**).

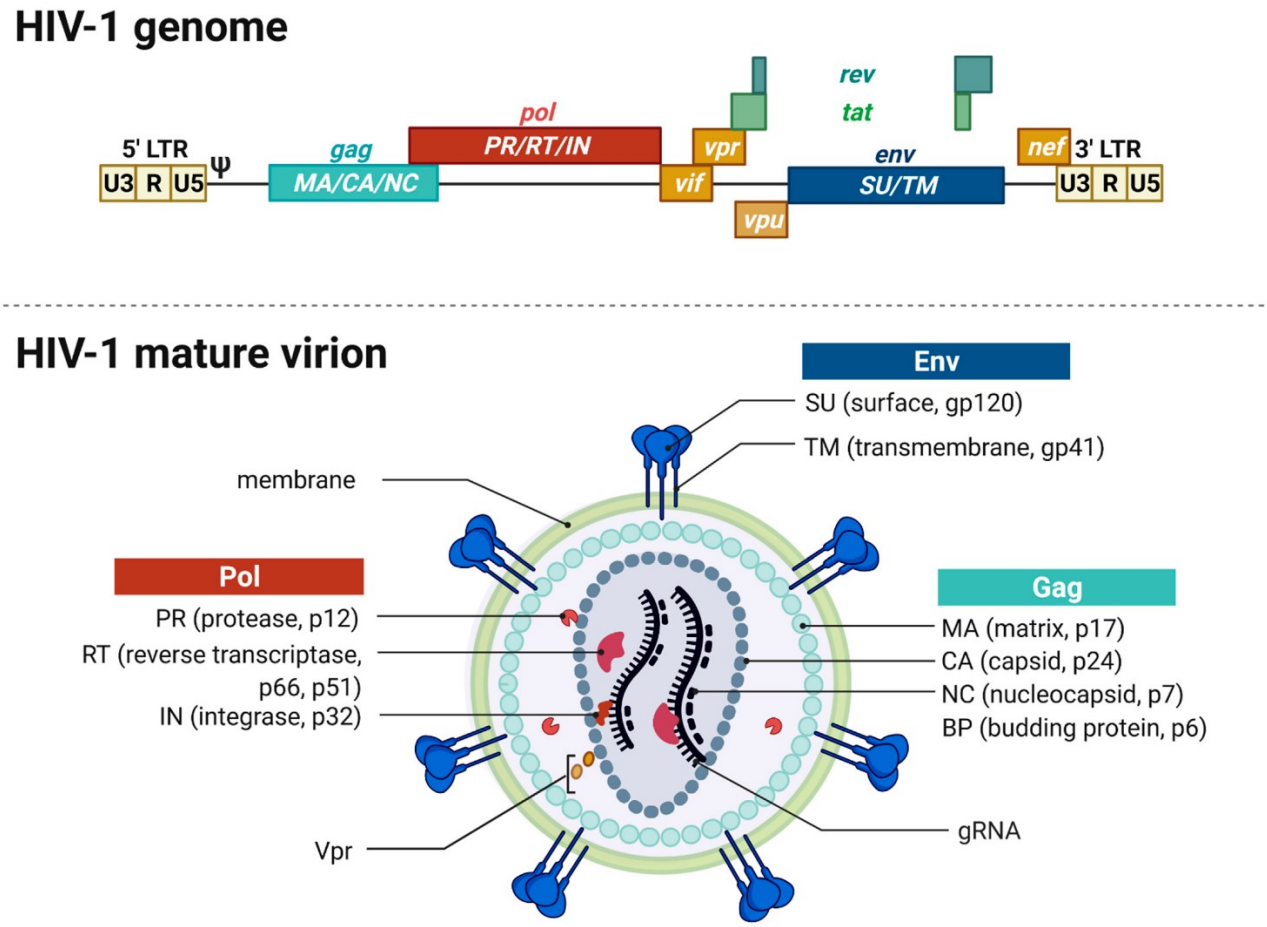

***Figure 5**: HIV-1 genome structure and virion organization (adapted by Heuvel et al., 2022)*

2.3 HIV-1 life cycle

The intracellular replication cycle of HIV-1 has a duration of around 1-2 days, although the exact duration and yield of viral production depend on the infected cell type and the relative activation state (Perelson *et al.*, 1996). HIV-1 preferentially infects Langerhans cells and dendritic cells of the mucosal tissue (primary viremia), then disseminates to regional lymphoid tissue. During the first days after infection, the initially infected cell population expands to produce a primary virus reservoir that later spreads systemically to the lymphoid organs and the bloodstream. The most permissive target cells are the CD4-receptor positive ($CD4^+$) lymphomonocytic lineage, which includes T lymphocytes, dendritic cells and monocytic/macrophagic cells like microglia and astrocytes (Chen *et al.*, 2022a). Because of the high number and susceptibility of target cells, viral

replication picks up speed and causes high plasma viremia (secondary viremia) (Zhang *et al.*, 2004; Miller *et al.*, 2005). Similarly to other viruses, the HIV-1 replication cycle can be separated into different phases: attachment and entry, reverse transcription, nuclear import and integration, viral gene expression, assembly of viral particles, budding and virion maturation (**Figure 6**).

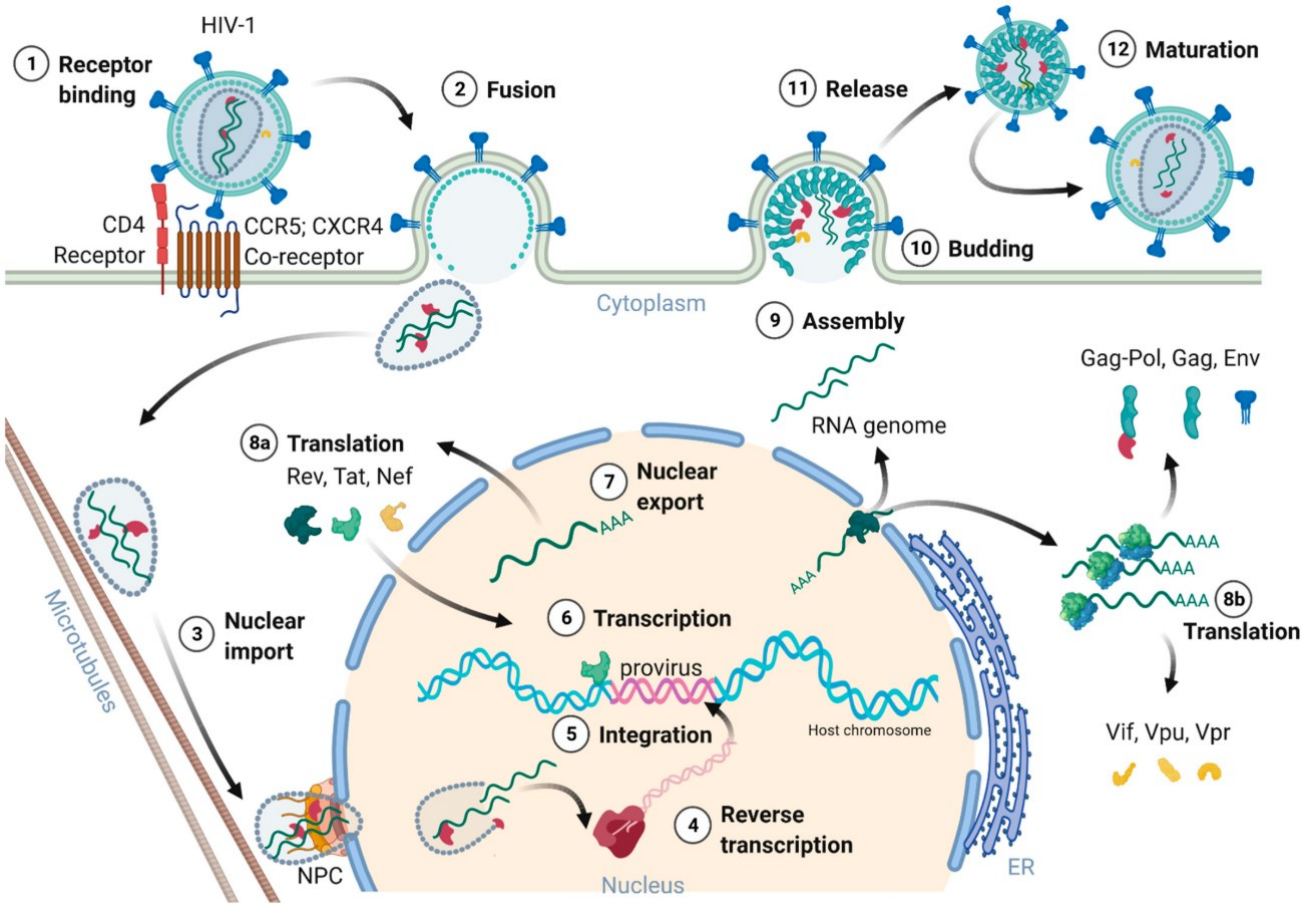

***Figure 6**: HIV-1 life cycle (adapted by Heuvel et al., 2022)*

The attachment involves the interaction between the viral surface gp120 protein and the host cell CD4 receptor (Turner and Summers, 2001; Freed, 2002). This receptor is a 60 kDa transmembrane glycoprotein consisting of four Ig-like extracellular domains and a cytoplasmatic tail which interacts with the tyrosin-protein kinase Lck. CD4 acts as coreceptor during the major histocompatibility complex class II (MHC-II) and T-cell receptor (TCR) bound when adaptive immunity and antigen-presenting cells (APC) engage (Li, Yin and Mariuzza, 2013). The interaction

between the gp120 protein and the CD4 receptor is essential but not sufficient for the virus entry, since further contacts between the viral envelope and cell coreceptors need to occur to induce membrane fusion. The most widely used coreceptors are the C-X-C chemokine receptor 4 (CXCR4), which is predominantly expressed by hematopoietic cells, thymocytes and both memory and naïve T cells, and the C-C chemokine receptor 5 (CCR5), that primarily resides on the dendritic cells, macrophages, memory and naïve T cells. Under physiologic conditions, CCR5 acts as receptor for the MIP-1α (macrophage inflammatory protein-1α), MIP-1β (macrophage inflammatory protein-1β) and for the CC-ligand-5 (CCL5) RANTES, while the CXCR4 receptor (also called fusin or LESTER, leukocyte expressed seven-transdomain receptor) acts as the chemokine SDF-1 (stromal cell-derived factor-1) receptor (Doms and Peiper, 1997; Berger, Murphy and Farber, 1999). The viral entry is a multistep process that is triggered by the establishment of the gp120-CD4-coreceptor ternary complex. After a series of rearrangements in conformation, viral gp41 is inserted in the host cell membrane, thus promoting the fusion with the viral membrane (Wyatt *et al.*, 1998; Guttman *et al.*, 2012). Reverse transcription of the viral genomic RNA is largely completed during the migration of the viral capsid along the microtubule-associated proteins towards the nuclear pores, and finished during nuclear import(Müller *et al.*, 2022). Reverse transcription involves the transcription of the viral genomic RNA into the complementary DNA (cDNA) by the RT enzyme and comprises of three primary steps: (i) the RT RNA-dependent DNA polymerase activity creates the first strand of DNA (negative polarity) that is complementary to the viral RNA; (ii) the RNase H domain degrades the RNA template from the RNA-DNA hybrid molecule; (iii) DNA-dependent DNA polymerase activity of RT generates the complementary (positive polarity) DNA strand thereby forming the double-stranded viral cDNA. Reverse transcription ends in the cell nucleus where the capsid is disassembled (Müller *et al.*, 2022). The integration process starts when the linear double-stranded viral DNA associates with viral integrase and other viral and cellular proteins in a pre-integration complex (PIC). The integrase covalently inserts the 3'-OH ends of the viral DNA into the cell genome by joining to the 5'-phosphate ends of the nuclear DNA. This strand interchange leaves a 5-base single-strand gap for each junction and a 2-base overhang to the 5' end of the viral DNA, which are corrected by specific cell enzymes (Pommier, Johnson and Marchand, 2005). Although integration sites have not specific location on the host cell genome,

preferential integration has been found over transcriptionally active cell genome regions due to the higher accessibility (Zhang, Dornadula and Pomerantz, 1998; Schröder *et al.*, 2002).

The integration step is crucial for HIV-1 latent infection establishment since proviral DNA is permanently incorporated into the cellular host genome. Most cells contributing to the HIV-1 viral reservoir are resting memory $CD4^+$ T lymphocytes, but HIV-1 can also infect activated $CD4^+$ T cells which may subsequently revert to the resting memory state, downregulating viral transcription level and evading immune system-mediated cytotoxicity (Chen *et al.*, 2022b). Studies have shown that the removal of the activation stimulus from infected primary $CD4^+$ T cells also decrease cell activation but does not necessarily inhibit the viral transcriptional activity (Mohammadi *et al.*, 2014). Moreover, HIV-1 integration site selection likely contributes to latency establishment. According to the stochastic gene expression theory, random mutations affecting critical regulatory regions such as the *Tat* gene can impede active viral transcription, rendering latency independent of the host cell activation state (Vanhamel, Bruggemans and Debyser, 2019). For productive infection, transcription of viral mRNA is directed by the promoter in the 5' LTR's U3 region that acts together with cellular transcription factors, notably NF-κB, and viral transcription factors like Tat and Rev, the former functioning to increase the transactivation of LTR-driven transcription of the virus and the latter to enhance the RNA export and availability (Turner and Summers, 2001). A highly regulated splicing mechanism is used by HIV-1 to produce more than 30 unique mRNA isoforms. Main early gene products are the Tat, Rev, and the Nef proteins that accelerate viral transcription and mRNA export to the cytoplasm.

Virion assembly takes place inside the inner side of the plasma membrane, where the genomic RNA packages with nucleocapsid proteins. The gp160 Env polyprotein is glycosylated in the endoplasmic reticulum and delivered by vesicular transport to the cell membrane for addition to new virions. Budding releases immature viral particles acquiring the lipid membrane composed of cholesterol- and glycolipid-rich patches of the host cell plasma membrane that expresses viral glycoproteins (gp120 and gp41) and cellular proteins such as MHC antigens and cell adhesion molecules like ICAM-1 and cyclophilin A. These cellular components are probably responsible of improving the virion's infectivity, enhancing the attachment and fusion to the target plasma membrane cells (Nguyen and Hildreth, 2000). The maturation of viral particles occurs after budding and is the result of the proteolytic cleavage of the Gag and Gag-Pol polyproteins by the

viral PR, which produces the final mature structural components and enzymes necessary for the subsequent round of infection.

2.4 HIV-1 transmission route and pathogenesis

The main routes of HIV-1 transmission are sexual, parenteral and vertical. Among these, sexual transmission is by far the predominant route worldwide. HIV-1 has been isolated from both semen and female genital secretions as free virions or within infected cells. Transmission occurs via heterosexual or homosexual contact, with a proportional link between infection risk and number of sexual contacts. The estimated risk of transmission through heterosexual intercourse is generally lower than the homosexual one (0.1-0.2 % vs. 0.8 %, respectively) (Catania *et al.*, 1995). In low-income countries, heterosexual transmission prevails and infection risk is enhanced by genital mucosal or cutaneous lesions that recruit lymphocytes and monocytes to the infection sites, facilitating viral entry. Like other sexually transmitted illnesses, uncircumcised men are at greater risk for HIV-1 infection (Sharma *et al.*, 2018). Parenteral transmission occurs most frequently among intravenous drug users, transfusion recipients, haemophiliacs and high-risk professionals involved in practices such as medical or dental care, surgery and tattooing or piercing with contaminated equipment (WHO Fact Sheets, https://www.who.int/news-room/fact-sheets/detail/hiv-aids).

Vertical transmission occurs when the virus is passed from an infected mother to her child. This can happen *in utero* across the placenta, *peripartum* during delivery or *postpartum* through breastfeeding. The risk of vertical transmission is strictly connected to maternal clinical parameters such as viral load and $CD4^+$ T cell count. Although untreated women may transmit the infection to the child in 25% to 60% of the cases, effective antiretroviral treatment during pregnancy, prophylactic treatment of the newborn and the use of infant formula feeding may significantly reduce the risk of mother-to-child transmission (Teasdale, Marais and Abrams, 2011).

The course of natural history of HIV-1 infection can be divided into three phases with distinct characteristics: acute or initial phase, clinical latency or chronic asymptomatic stage and AIDS stage, the latter characterized by opportunistic infections, AIDS-associated cancers and neurological complications (**Figure 7**).

The acute infection has an incubation period of about three to six weeks during which there are either few or no symptoms, usually limited to a mild symptomatic syndrome lasting two weeks. Clinical manifestations in the meantime are usually indistinguishable from mononucleosis or a flu-like illness and include fever, lethargy, fatigue, sore throat, skin rash, myalgia, headache, lymphadenopathy, mouth ulcers and, less commonly, oral candidiasis and meningoencephalitis (*HIV and AIDS: The Basics; HIV.gov*, 2025). During this phase, $CD4^+$ T cells count drops and $CD8^+$ T cells rise, resulting in an unbalanced CD4:CD8 ratio (<1).

During primary infection, the titres of both plasma and cellular virus rise sharply, with plasma viremia levels reaching 10^6 to 10^8 copies/mL. The initial low to moderate viral load results from early viral replication in local lymph nodes. The migration of infected $CD4^+$ T cells through the bloodstream to major lymphoid tissues such as gastrointestinal Peyer's patches, spleen and bone marrow, leads to secondary infection of highly susceptible target cells (Simon, Ho and Abdool Karim, 2006).

The length of this latency or asymptomatic period is highly variable and affected by several factors, including the viral expansion during the primary infection, phenotypic characteristics of the viral strain and host immune competence. Disease monitoring during this stage focuses on measuring the number of $CD4^+$ T lymphocytes and plasma viral load. If the absence of treatment, viral load gradually increases over time, while $CD4^+$ T cell levels progressively decline. Despite this immunocompromised state, a $CD4^+$ T count >300-350 cells/mm^3 may prevent the onset of severe clinical symptoms. However, progressive impairment of the immune system increases the susceptibility to opportunistic infections, ranging from complete absence of symptoms to the evolution of intermittent or chronic nonspecific manifestations.

Recurrent relapses of *Herpes simplex* virus infection, prolonged recovery from common illnesses and persistent fatigue can be manifestations of immunity breakdown and thus need to be clinically investigated. The advanced AIDS phase is characterized by a $CD4^+$ T cell count <200 cells/mm^3, leading to the loss of the immune system control. Indeed, opportunistic infections such as visceral toxoplasmosis, *Pneumocystis jirovecii* infection, pneumonia, cytomegalovirus infection, oesophagus candidiasis, disseminated atypical mycobacteriosis and malignancies, including Kaposi's sarcoma and primary central nervous system lymphoma, are usually observed in patients

during this stage (*HIV and Opportunistic Infections - HIV.gov*, 2025). When patients are not treated or not responsive to antiretroviral therapy, this condition can lead to death.

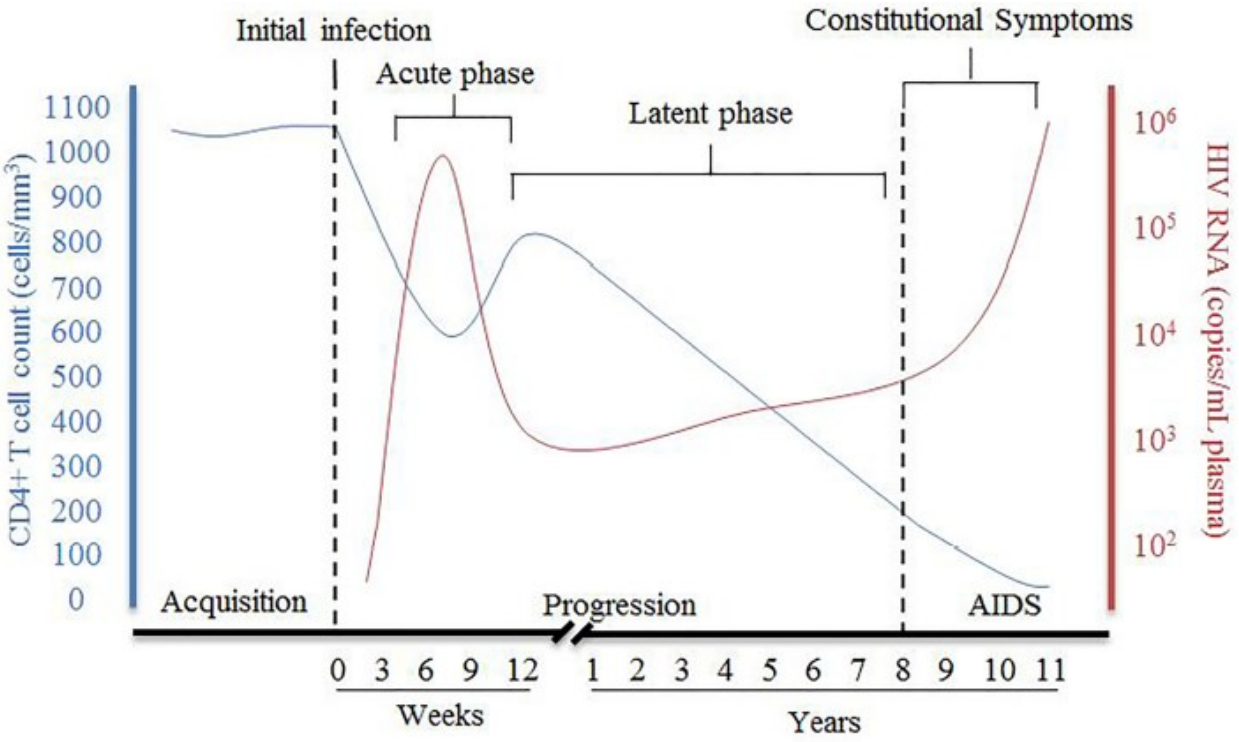

***Figure 7**: HIV-1 infection phases (adapted by Tough et al., 2019)*

2.5 HIV-1 genetic variability and subtypes

The unique genetic diversity of HIV is a virus hallmark property that strongly influences cellular tropism, patterns of transmission, virus-host interactions and ultimately the clinical course of infection (Blackard, Cohen and Mayer, 2022). This deep polymorphism is primarily a consequence of two conditions: the incredibly high error rate of nucleotide incorporation by the viral RT, which is estimated at approximately 3.4 x 10^5 substitutions per replication cycle (Taylor et al., 2008), and the very high viral replication rate with more than 10^{10} virions being generated each day (Coffin, 1995; Perelson *et al.*, 1996).

Phylogenetic analysis categorize circulating HIV-1 strains in four groups: M (Main or Major), N (non-M/non-O), O (Outlier), and P. Groups N and O remain largely restricted to Central-Western African

locations, in particular Gabon and Cameroon regions where the chimpanzee *Pan troglodytes troglodytes* is naturally distributed (Peeters *et al.*, 1997). Group P was first identified in 2009 in a human isolate highly related to *SIVgor* isolates, although the origin remains to be established. To date, HIV-1 group P has been identified in only two patients (Plantier *et al.*, 2009; Sauter *et al.*, 2011).

Group M is responsible for approximately 95% of all global HIV-1 infections and represents the origin of the current pandemic. It is further divided into ten subtypes or clades: A-D, F-H, J, K, and L, some of which have distinctive geographical distributions. Superinfection or co-infection with strains from multiple subtypes, followed by recombination, can result in the development of mosaic viruses known as circulating recombinant forms (CRFs). The classification as CRF derived from the identification of at least three distinct recombination events, while the epidemiologic significance depends on relative replicative fitness or host adaptability.

Although representing approximately 11.3% of all HIV-1 infections globally, subtype B is most prevalent in the Americas, Western and Central Europe, where most therapeutic and clinical research are conducted. Subtype C is the most prevalent globally, accounting for 50.4% of infections, with a higher prevalence in Southern and Eastern Africa, Ethiopia and India, followed by subtype A (12.4%), CRF02_AG (6.6%), CRF01_AE (5.4%), subtype G (2.9%) and subtype D (2.6%). The remaining subtypes (F, H, J, and K) and all the circulating URFs and CRFs are responsible for approximately 8% of total infections (Nair *et al.*, 2024) (**Figure 8**). In 2019, a new subtype L was identified in the Democratic Republic of Congo, representing the first new subtype designation since the year 2000, when all previously known subtypes were officially declared (Buonaguro, Tornesello and Buonaguro, 2007).

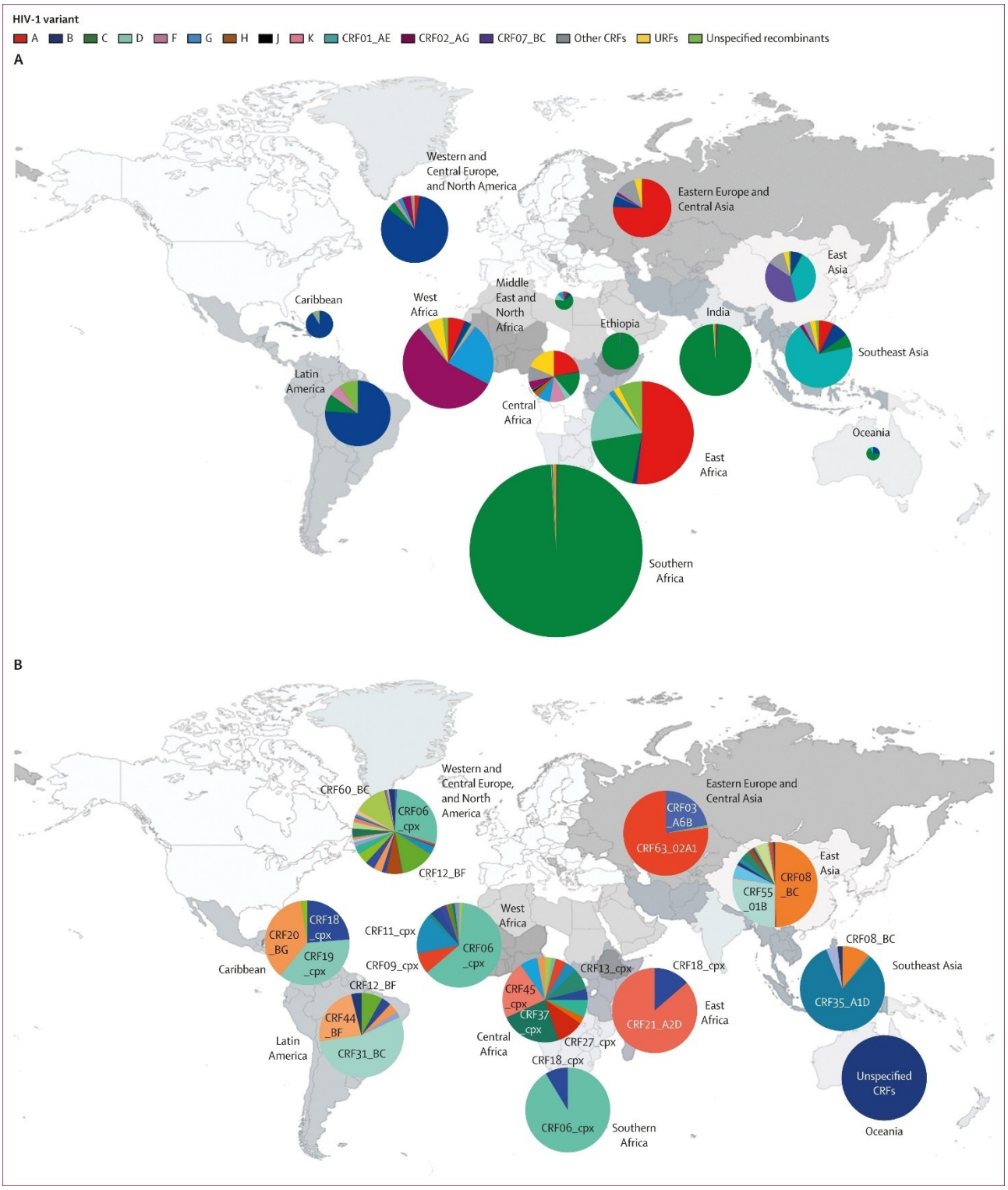

Figure 8: *HIV-1 variants global distribution based on subtype (A) and CRFs (B) (adapted by Nair et al., 2024)*

Both HIV-1 and HIV-2 cause AIDS, even though HIV-1 has increased pathogenicity and transmissibility (Nyamweya *et al.*, 2013). At the molecular level, amino acid sequences of the viral envelope glycoproteins exhibit significant divergence: 25% to 35% between subtypes and up to 20% within a single subtype. In the same way, HIV-2 strains comprise six phylogenetic lineages (A to H), and they possess the same extent of genetic diversity as HIV-1, with up to 25% divergence in the *Gag*, *Pol* and *Env* genes. HIV-1 and HIV-2 are around 55-60% genetically different, with an almost identical genome organization except for one accessory gene (*Vpu* in HIV-1 and *Vpx* in HIV-2) (Ayinde *et al.*, 2010).

2.6 Antiretroviral drug classes and therapies options

The management of HIV-1 infection relies exclusively on combined Antiretroviral Therapy (cART), the only effective way to avoid disease progression. Since the advent of zidovudine (AZT) in 1987, more than forty individual antiretroviral compounds have been approved by the U.S. Food and Drug Administration (FDA) and the European Medicines Agency (EMA) (**Figure 9**). Antiretroviral agents are grouped and classified into 8 different classes based on mechanism of action (*HIV Drug Classes - Fact sheets; HIV.gov*, 2025):

- Non-Nucleoside Reverse Transcriptase Inhibitors or NNRTIs
- Nucleoside Reverse Transcriptase Inhibitors or NRTIs
- Protease Inhibitors or PIs
- Fusion Inhibitors or FIs
- CCR5 Antagonists or CAs
- Attachment Inhibitors or AIs
- Integrase Strand Transfer Inhibitors or INSTIs
- Capsid Inhibitors or CIs

FDA Approval of HIV Medicines

1981: First AIDS cases are reported in the United States.

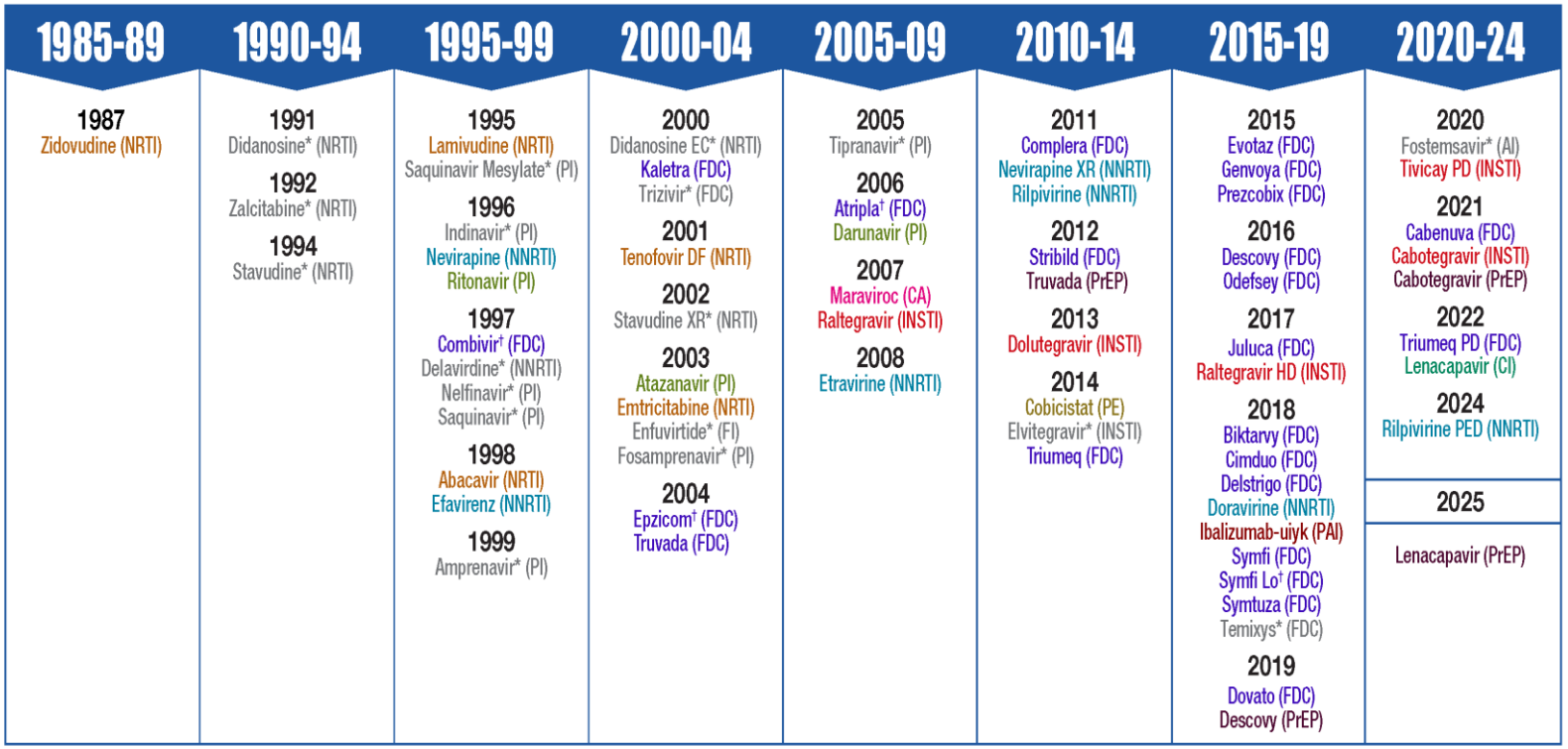

Drug Class Abbreviations:
AI: Attachment Inhibitor; **CA:** CCR5 Antagonist; **CI:** Capsid Inhibitors; **FDC:** Fixed-Dose Combination; FI: Fusion Inhibitor; **INSTI:** Integrase Inhibitor; **NNRTI:** Non-Nucleoside Reverse Transcriptase Inhibitor; **NRTI:** Nucleoside Reverse Transcriptase Inhibitor; **PE:** Pharmacokinetic Enhancer; **PI:** Protease Inhibitor; **PAI:** Post-Attachment Inhibitor; **PrEP:** Pre-exposure prophylaxis

Note: Approvals are for HIV treatment, unless otherwise indicated.
*Drugs in gray are no longer available and/or are no longer recommended for use in the United States by the HHS HIV/AIDS medical practice guidelines. These drugs may still be used in fixed-dose combination formulations.
†Fixed-dose combination brand products that are available as generic only.

For more information, visit HIVinfo.NIH.gov.

HIVinfo.NIH.gov

Figure 9: *FDA HIV-1 drugs approval timeline, HIV.gov*

NNRTIs inhibit reverse transcription by binding within a hydrophobic pocket near the catalytic site of the viral polymerase, causing conformational changes and preventing enzymatic activity (Arts and Hazuda, 2012). Six NNRTIs are now licensed for clinical use in combination antiretroviral regimens: doravirine (DOR), efavirenz (EFV), etravirine (ETR), rilpivirine (RPV), nevirapine (NVP) and delavirdine (DLV). NPV and DLV use is now no longer recommended due to inferior potency, less convenient dosing intervals and more common drug-drug interactions compared with newer NNRTIs. EFV is still used, but only in resource-limited settings or when other preferred drugs are unavailable.

Differently from NNRTIs, NRTIs are phosphorylated intracellularly to their diphosphate or triphosphate metabolites, which interfere with viral replication by competitively inhibiting the binding of cellular deoxynucleotide phosphates (dNTPs) into new cDNA. Competition leads to chain termination during reverse transcription elongation. Among the approved NRTIs, tenofovir disoproxil fumarate (TDF), tenofovir alafenamide (TAF), emtricitabine (FTC), abacavir (ABC) and lamivudine (3TC) are most frequently used as backbone drugs in antiretroviral treatment regimens, while older NRTI such as AZT, didanosine or zalcitabine are no longer used.

Protease Inhibitors (PIs) are peptidomimetics which act on the late stage of viral life cycle by preventing proteolytic cleavage of gag and gag/pol precursor polyproteins. Interference with the viral PR results in aberrant virions' maturation, leading to the release of non-infectious viral particles (Wensing, van Maarseveen and Nijhuis, 2010). FDA-recommended PIs include atazanavir (ATV), atazanavir/cobicistat (ATV/c), darunavir (DRV), darunavir/cobicistat (DRV/c), and lopinavir/ritonavir (LPV/r), while other PIs such as fosamprenavir (FPV), indinavir (IDV), nelfinavir (NFV), ritonavir (RTV), saquinavir (SQV) and tipranavir (TPV) are no longer used.

The only FI enfuvirtide (T20) approved for clinical use acts by binding to the heptad repeat 1 (HR1) region of gp41, thereby inhibiting the formation of the six-helix bundle required for viral and cellular membrane fusion (Dando and Perry, 2003).

Maraviroc (MVC) is the only CCR5 antagonist approved for clinical treatment and is used only among CCR5-tropic viral strain-infected patients (Sayana and Khanlou, 2009).

Fostemsavir (FTR), the prodrug of the active compound temsavir (TMV), is a recently approved AI that binds directly to the gp120 envelope glycoprotein, trapping it in a conformation that precludes

exposure of the V3 loop necessary for interaction with the CCR5 and CXCR4 coreceptors (Seval, Frank and Kozal, 2021).

Ibalizumab (IBA), approved in 2018, is the first-in-class post-attachment inhibitor. It is a humanized monoclonal antibody that binds to specific residues of domain 2 of the CD4 receptor without interacting with the MHC class II molecule and gp120 binding sites. This differential binding enables IBA to block HIV entry without affecting MHC class II-mediated immune function or causing the generation of HIV-induced syncytia among infected and uninfected $CD4^+$ cells. Although IBA does not interfere with gp120 binding to CD4, it interrupts the following assembly of the gp120/CD4 complex and engagement with coreceptors, thereby inhibiting viral entry and fusion (Markham, 2018).

INSTIs block HIV-1 IN function, which mediates integration of proviral DNA into the host genome, avoiding the strand transferring on the host DNA (Smith *et al.*, 2021). Since 2007, five agents have been approved in this class: raltegravir (RAL), elvitegravir (EVG), dolutegravir (DTG), bictegravir (BIC) and cabotegravir (CAB). The last three agents are the most recent generation of INSTIs and possess high potency, high genetic barrier to resistance and very good tolerability profiles and hence are the drug of choice for both first line and switch therapeutic regimens (Scarsi *et al.*, 2020).

Lenacapavir (LEN) is the first-in-class CI and last HIV-1 inhibitor approved by the EMA and FDA in December 2022. It inhibits multiple steps of viral life cycle such as capsid-mediated nuclear import of PIC, virion assembly and capsid maturation (Dvory-Sobol *et al.*, 2022).

In recent years, many more drug-combined formulations were licensed to optimize ART regimens improving safety, pharmacokinetic and drug-drug interaction, leading to the development of new treatment's strategies, such as pre-exposure prophylaxis (PrEP). First approved in 2012, PrEP is particularly indicated for individuals who have sex with partners with HIV with an unknown or detectable viral load, people who don't use condoms or people who do injectable drugs and share needles and equipment (EACS guidelines v13.0, 2025). As of today, four formulations have been licensed: two everyday pills (Truvada® and Descovy®) and two long-acting injections (Apretude® and Yeztugo®). Safety and efficacy of these formulations were further measured in a meta-analysis which considered 15 oral PrEP-based random clinical trials including all the populations at risk: no differences, directly correlated with adherence, where observed between the treatment and control arms (Murchu *et al.*, 2022).

2.7 Multidrug-resistant HIV-1 treatment and clinical options

MDR remains one of the most significant challenges in contemporary clinical management, including HIV-1 infection. Despite the availability of highly effective ART options, drug-resistant HIV-1 may substantially compromise the efficacy of ART, increasing the risk of HIV transmission, as well as HIV-related morbidity and mortality.

A retrospective assessment of 15,628 plasma genotypic resistance tests collected from January 1998 to December 2012 in 6,802 ART HTE individuals demonstrated a two-thirds reduction in overall resistance to any antiretroviral drug class. The reduction is likely attributable to improved clinical management of HIV-1 disease, ongoing improvement in antiretroviral drugs in terms of potency, efficacy, tolerability and genetic barrier, and early treatment intervention upon virological failure. Despite these improvements, resistance to at least one drug class remained stable around 50% of the viral sequences collected between 2011 and 2018, while the rate of MDR also levelled off at 9% between the same years, compared to a maximum of 17% observed over the previous two decades. Interestingly, prior prolonged exposure to ART was associated with a higher risk of selection of MDR virus, whereas patients who initiated first-line ART in 2008 had a lower likelihood of development of multidrug resistance (Lombardi et al., 2021).

Other evidence indicates that "functional" monotherapy, resulting from fluctuations in drug half-lives or non-adherence, can allow the selection of resistant viral populations even within otherwise effective triple-drug regimens. While combination therapy is expected to reduce viral replication and prevent resistance, achieving viral suppression remains challenging in some cases. This difficulty may be partly due to nonuniform distribution of drugs within anatomical compartments, leading to tissue subtherapeutic concentrations in certain areas and the consequent occurrence of resistant strains (Feder et al., 2021).

In cases of virological failure, European AIDS Clinical Society (EACS) guidelines recommend that at least two, preferably three, fully active antiretroviral drugs should be administered to patients with historical and current genotypic resistance data guiding the choice. Salvage therapy key principles include: in case of limited NRTI mutations (e.g., M184V and/or 1-2 TAMs), the new regimen should include two NRTIs (3TC or FTC and TDF or TAF) and one active PI/b (e.g., DRV/b) or a second-generation INSTI (BIC or DTG); if the genotype assay highlights multiclass resistance (≥ 2

classes), treatment must include a minimum of one fully active PI/b (e.g., DRV/b) or one fully active second-generation INSTI (BIC, DTG), and one or two other drugs fully active (e.g., NRTIs and/or DOR) and/or drugs from previously unused classes (INSTI, NNRTI, PI/b), based on genotypic testing; if in a two- to three-drug active regimen is not possible to use NRTIs, NNRTIs, PI/b or INSTIs, then drugs with a novel mechanism of action, such as FTR, IBA and LEN may be added to achieve the two- to three-drug active regimen. In any case, monotherapy treatment is not recommended.
In conclusion, successful care of HIV-1 MDR patients requires the delivery of maximally effective antiretroviral regimens, optimal adherence strategies as well as regular viral load monitoring to check the treatment efficacy and/or switch to a more adapt drug regimen in case of virological failure (HIV-viral load >200 copies/mL).

2.7.1 The use of Lenacapavir to manage MDR patients

Lenacapavir (LEN, brand name Sunlenca®), as mentioned in **paragraph 2.6**, is the first-in-class capsid inhibitor approved in 2022 for the treatment of MDR HIV- infections. LEN has a multistep mechanism of action including (i) the stabilization of viral capsid cores in cytoplasm, blocking nuclear import of viral DNA; (ii) the inhibition of the interactions between capsid core and both Nup153 and CPSF6 cellular cofactors, essential for nuclear import; (iii) the assembly of CA hexamers during capsid core formation and virion maturation. Virions produced in presence of LEN present capsid modifications that prevent new cells entry (Bester *et al.*, 2020; Hitchcock *et al.*, 2024) (**Figure 10**).

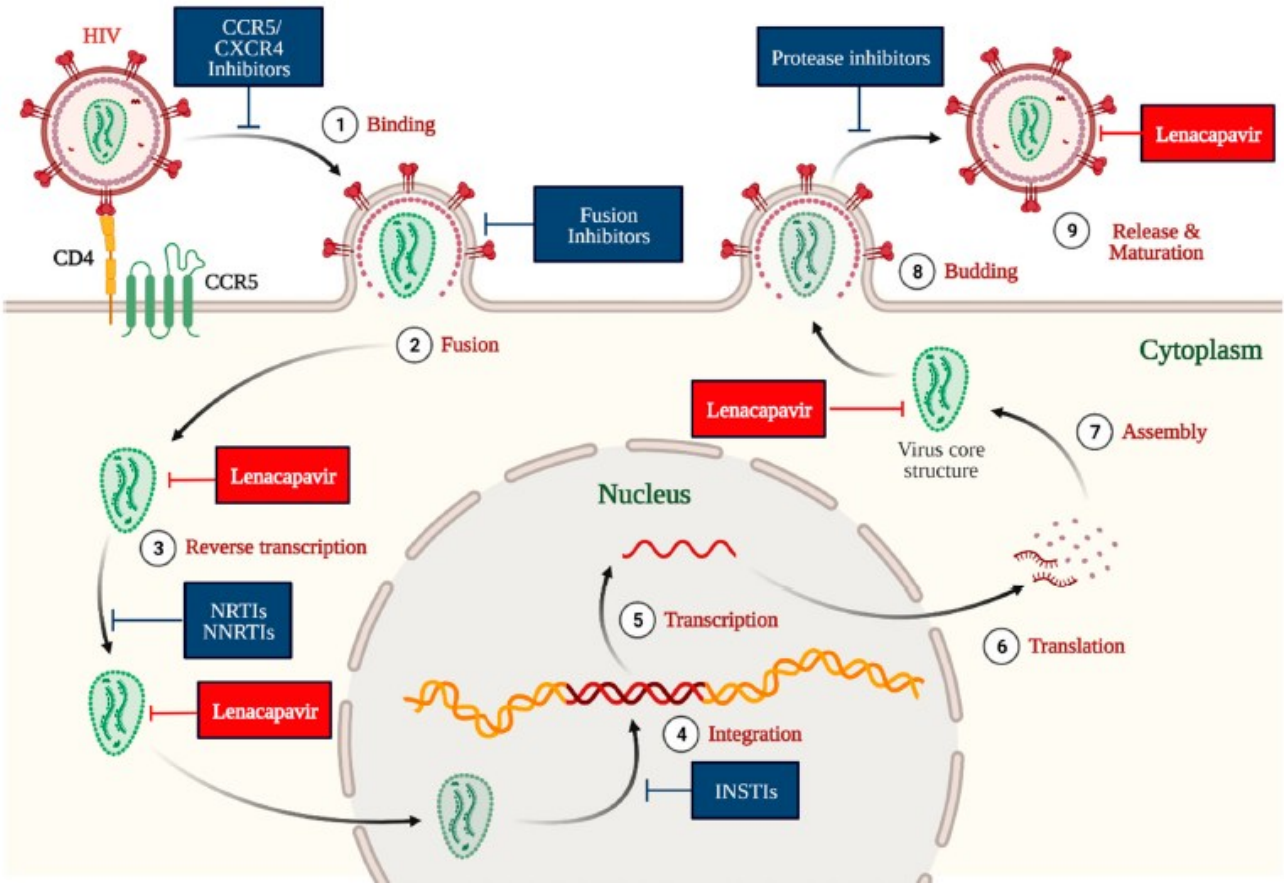

***Figure 10**: Lenacapavir multistep mechanism of action (adapted by Dzinamarira et al., 2023)*

In vitro, LEN showed a high potent efficacy against HIV-infected primary macrophages/monocytes and $CD4^+$ T lymphocytes, with a half-maximal effective concentration (EC_{50}) of 56 and 32 pM, respectively (Link *et al.*, 2020). Curiously, LEN affects multiple sequential steps in a dose-dependent manner: at 0.5 nM, LEN inhibits integration without affecting reverse transcription; at 5 nM, viral DNA levels are reduced in both cytoplasm and nucleus, confirmed by the reduced amount of 2-LTR circles; at 50 nM, reverse transcription is also impaired (Bester *et al.*, 2020). In infected MT-4, LEN showed a EC_{50} of 150 pM, which is lower than that of many antiretroviral drugs, including RPV, EFV, DTG, BIC, ATV, DRV and TAF. Comparable LEN efficacy was observed across all HIV-1 groups (including A, A1, AE, AG, B, BF, C, D, E, F, G and H subtypes) and against two HIV-2 isolates, with a 15- to 25-fold lower activity (EC_{50} 885 pM) as compared to HIV-1 (Hitchcock *et al.*, 2024).

In vivo, oral LEN has shown a median time to maximal plasma concentration (T_{max}) of 4 hours and a plasma half-life of 10-12 days. The single-dose pharmacokinetics of oral LEN administration are

non-linear and less than dose proportional over the dose range of 50 to 1800 mg. The bioavailability is low (6-10%) and unaffected by diet. Differently, subcutaneously injectable (SC) LEN has displayed two-phase absorption kinetics, with an initial fast-release absorption phase followed by a slow-release absorption phase. This behaviour affects the half-life due to the elimination rate, which is faster than the absorption rate. After a single SC dose of 30-450 mg, T_{max} is reached after 77-84 days, with a plasma half-life of 8-12 weeks, leading to a dosing interval of 26 weeks.

Regarding the distribution, LEN is highly protein-bound (>99.8%), with a volume of 976 L based on population pharmacokinetic analysis. The clearance of LEN is mainly mediated by faecal excretion, with a negligible renal elimination. From a metabolic point of view, LEN is a substrate of cytochrome P450 (CYP) 3A4, uridine diphosphate glucuronosyltransferase (UGT) 1A1 and p-glycolprotein (P-gp). Since the CYP3A4 is involved in the metabolism of many other drugs, LEN long half-life could affect the exposure to them if initiated within 9 months after the last SC dose of it (Marzolini *et al.*, 2025). According to Sunlenca® prescription information (https://www.gilead.com/-/media/files/pdfs/medicines/hiv/sunlenca/sunlenca_pi.pdf), the therapeutic regimen administration can be initiated following two options (**Figure 11**):

- Option 1:

  Initiation dosage

  - On day 1, 927 mg by SC injection or 600 mg orally
  - On day 2, 600 mg orally

  Maintenance dosage (every 6 months (26 weeks)) +/- 2 weeks

  - 927 mg by SC injection

- Option 2:

  Initiation dosage

  - On day 1, 600 mg orally
  - On day 2, 600 mg orally
  - On day 8, 300 mg orally
  - On day 15, 927 mg by SC injection

  Maintenance dosage (every 6 months (26 weeks)) +/- weeks

- 927 mg by SC injection

If a scheduled maintenance injection cannot be administered for more than two weeks (from the 26 to 28 weeks), Sunlenca® 300 mg tablets may be taken once every seven days for up to 6 months until the regular SC injections resume. If the missed period is longer than 28 weeks, the patient must reinitiate with first or second option before maintenance SC injection dosing. In every case, SC injections doses must be administered only by healthcare providers, and potential adverse events (post SC injection and during maintenance doses) must be communicated immediately (*Sunlenca prescription label*, no date).

***Figure 11**: Sunlenca®'s administration dosage options (adapted by https://www.sunlencahcp.com/)*

Thanks to its multiple administration routes (oral or SC injectable) and variable dosing intervals, Lenacapavir is now the only FDA-approved drug for HIV-1 PrEP option offering six months of protection.

Specifically, LEN PrEP formulation (named Yeztugo®) efficacy and safety data come from phase 2 and 3 PURPOSE 1 (clinicaltrial.gov number: NCT04994509) and PURPOSE 2 (clinicaltrial.gov number: NCT04925752) clinical trials, respectively. In PURPOSE 1, twice-yearly SC LEN injection demonstrated 100% reduction in HIV-1 infections compared to once-daily FTC+TDF in 2,134 sub-Sahara African cisgender women, while in PURPOSE 2, only two HIV-1 infections were described among 2,179 cisgender men and gender-diverse participants undergoing twice-yearly LEN SC injection, resulting in a 99.99% of HIV-1 infection prevention compared to once-daily FTC+TDF. In both trials, Yeztugo® therapy demonstrated a higher efficacy in HIV-1 infection prevention compared to control group, with generally good toleration and no severe adverse events onset (Bekker *et al.*, 2024; Kelley *et al.*, 2025).

As previously stated, Lenacapavir use is recommended and indicated for MDR patients, specifically those who have limited treatment options. In the pivotal phase 2/3 CAPELLA clinical trial (clinicaltrial.gov number: NCT04150068), twice-yearly SC injected LEN has demonstrated a remarkable reduction in viral load during functional monotherapy, with an overall $CD4^+$ T cell count increase. Despite the limited cohort size, LEN was maintained in wide subgroups, including patients with integrase resistance or those on optimized background regimens (OBR) that included fewer than one fully active agent or DTG or darunavir DRV monotherapy. Interestingly, most HIV-1 variants with LEN resistance mutations exhibited decreased replication capacity, suggesting a fitness cost that would jeopardize their ability to sustain infection (Segal-Maurer *et al.*, 2022).

2.7.2 Lenacapavir-associated resistance

Despite the high efficacy of LEN in MDR patients' treatment, resistance-associated mutations (RAMs) have been observed in both treatment naïve and heavily-treatment experienced individuals. *In vitro* experimental data and clinical trial outcomes highlighted the emergence of major and accessory RAMs in the p24 capsid coding region at codons 56, 57, 66, 67, 70, 74, 105,

and 107 (**Table 1**), without impacting on other drug classes susceptibility (Margot *et al.*, 2021). These RAMs seemed to decrease LEN susceptibility in PBMCs by 6 to 3,200-fold compared to wild-type virus (Link *et al.*, 2020). *In vivo*, different polymorphic mutations were found in 2,031 treatment-naïve people with HIV (PWH) in resistance-associated positions such as M66C (4.18%), Q67K (3.84%), N74R (2.81%) and T107L (4.03%) (Nka *et al.*, 2023). Another *in vivo* study which analysed the incidence of Lenacapavir RAMs in a treatment-naive cohort in Uganda observed a prevalence of the polymorphic mutation L56M in almost half of the sampling (258/546, 47.3%), principally in A1 subtype (87.2%), suggesting that natural polymorphisms in resistance-associated positions could be detected in subpopulation based on geographical region and viral subtype (Omoding *et al.*, 2025) (**Table 2**).

RAM	Mutation Type	Selection context	Natural polymorphism
L56I	**Major**	***in vitro***	**L56M[1]**
N57S	**Accessory**	***in vitro***	
M66I	**Major**	***in vitro/in vivo***	**M66C[2]**
Q67H	**Major**	***in vitro/in vivo***	**Q67K[2]**
K70N/H/R/S	**Major**	***in vivo***	
N74D	**Major**	***in vitro/in vivo***	**N74R[2]**
N74S	**Accessory**	***in vitro***	
N74K	**Major**	***in vivo***	
A105T/S	**Accessory**	***in vivo***	
A105E	**Accessory**	***in vitro***	
T107N	**Accessory**	***in vitro/in vivo***	
T107S/A/C	**Accessory**	***in vitro***	**T107L[2]**

***Table 2**: In vitro and in vivo resistance-associated mutations (RAMs) to Lenacapavir according to Stanford HIVdb version 9.8. [1-2]Mutations indicated as natural polymorphisms (threshold of ≥1% prevalence) ([1]data from Omoding et al., 2025; [2]data from Nka et al., 2023)*

In the phase 2 clinical trial CALIBRATE (clinicaltrials.gov number: NCT04143594), designed to evaluate the safety and efficacy of LEN in combination with other antiretrovirals, 3/157 of participants developed treatment-emergent RAMs. Notably, one participant developed both Q67H and K70R mutations at week 10 after the development of the M184V/I RT mutation while receiving SC LEN and FTC/TAF. The second participant with emergent resistance was on fully oral LEN +

FTC/TAF and developed the Q67H and K70R at week 54, highlighting suboptimal adherence through pill count and drug concentrations. The third participant developed Q67H and K70R mutations at week 80 while receiving SC LEN + TAF (Neverette *et al.*, 2025).

Concerning the CAPELLA study, at week 104 14 participants (19.4%) developed LEN-associated RAMs among which M66I (6 cases), Q67H (five cases), K70N/H (two cases) and N74D (one case), with half of the participants able to suppress viremia. Curiously, five of these individuals managed to reach this goal without changing their OBR (Ogbuagu *et al.*, 2025).

2.8 Aim of the research

HIV-1 inhibition and viral suppression is nowadays possible thanks to many active molecules, leading to the formulation of largely active therapeutic regimens, simplification strategies and long-acting approaches. Consequently, an easier drug administration and a viral transmission reduction have been reached, even in high-risk populations and low-income regions. Despite all, the treatment approach for MDR individuals remains challenging due to limited options to obtain an efficient drug regimen, adverse events caused by drug-drug interactions, poor adherence and coinfections. Lenacapavir, the first-in-class capsid inhibitor, is indicated for MDR patients thanks to its high potency and its multistep mechanism of action. It is under investigation for its open-ended administration routes (oral or injectable) and variable dosing intervals (daily to every two years), it is particularly indicated for patients who are adherence-challenged, thus moving beyond the daily oral dosing. Moreover, Lenacapavir-associated RAMs are well documented in literature, and they appear to only partially affect viral susceptibility when confirmed, even though resistances to drugs included in the OBR were observed (Ogbuagu *et al.*, 2025). For these reasons, this work focused on the *in vitro* characterization of Lenacapavir susceptibility and its genetic barrier in a small panel of subtype B and non-B HIV-1 strains, deriving from heavily-treatment experienced and treatment-naïve people with HIV.

3 MATERIALS AND METHODS

3.1 Eukaryotic cell lines

3.1.1 293-LX

The Lenti-X 293T cell line (293-LX, Takara Bio) derived from human embryonic kidney (HEK), transformed with Adenovirus type 5 DNA. This cell line is adherent, highly transfectable and supports high levels of viral protein expression. Simian virus (SV40) large T antigen, which is present in HEK 293 cells, enables them to produce high lentiviral titers (Gama-Norton *et al.*, 2011). Cells were maintained in Dulbecco's Modified Eagle's Medium High Glucose with L-glutamine (DMEM, EuroClone), supplemented with 10% of heat-inactivated Fetal Bovine Serum (FBS, EuroClone) and 1% of 100 U/mL penicillin and 100 µg/mL streptomycin (PS, EuroClone) in a humidified incubator at 37°C with 5% CO_2.

3.1.2 TZM-bl

TZM-bl cells (National Institute for Biological Standards and Control - NIBSC) derived from a clone of HeLa cells engineered to stably express CD4, CCR5 and CXCR4. The TZM-bl cell line was generated from JC.53 cells by introducing separate integrated copies of luciferase and β-galactosidase genes under the control of an HIV-1 promoter, allowing sensitive and accurate measurements of HIV infection (Wei *et al.*, 2002). TZM-bl adherent cell line was maintained in DMEM supplemented with 10% heat-inactivated FBS and 1% PS in a humidified incubator at 37° C with 5% CO_2.

3.1.3 U87-CXCR4

U87 cell line was isolated from a glioblastoma obtained from a 44-year-old female patient and genetically modified to express CXCR4 and CCR5 HIV-1 co-receptors (Princen *et al.*, 2004). U87 is an adherent cell line supporting high levels of viral replication. U87-CXCR4 (NIBSC) were maintained in DMEM supplemented with 10% heat-inactivated FBS, 1% PS, 300 µg/mL gentamicin (G418, Sigma-Aldrich) and 1µg/mL puromycin (Sigma-Aldrick) in a humidified incubator at 37°C with 5% CO_2.

3.1.4 MT-2

MT-2 cell line (NIBSC) derives from human T-cell transformed by co-cultivating with leukaemia lymphocytes harbouring HTLV-1. MT-2 cells are permissive for the infection and replication of HIV-1 X4-tropic strains and were used to enhance the viral titer of viruses obtained after transfection into 293-LX cells. This suspension cell line was maintained with Roswell Park Memorial Institute (RPMI 1640) medium (EuroClone) supplemented with 10% heat-inactivated FBS, 1% PS and 2 mM L-glutamine (EuroClone) in a humidified incubator at 37°C with 5% CO_2.

3.2 Plasmids and vectors

3.2.1 pNL4-3 plasmid

The source plasmid chosen as backbone to subsequently generate recombinant vectors and viruses was the pNL4-3 (**Figure 12**), obtained from NIH AIDS Reagent Program (www.aidsreagent.org). The 5' SmaI-EcoRI fragment of proviral NY5 (5' SmaI in flanking cellular DNA to 3' EcoRI) and the 3' fragment of proviral LAV (5' EcoRI to 3' NruI in flanking cellular DNA)

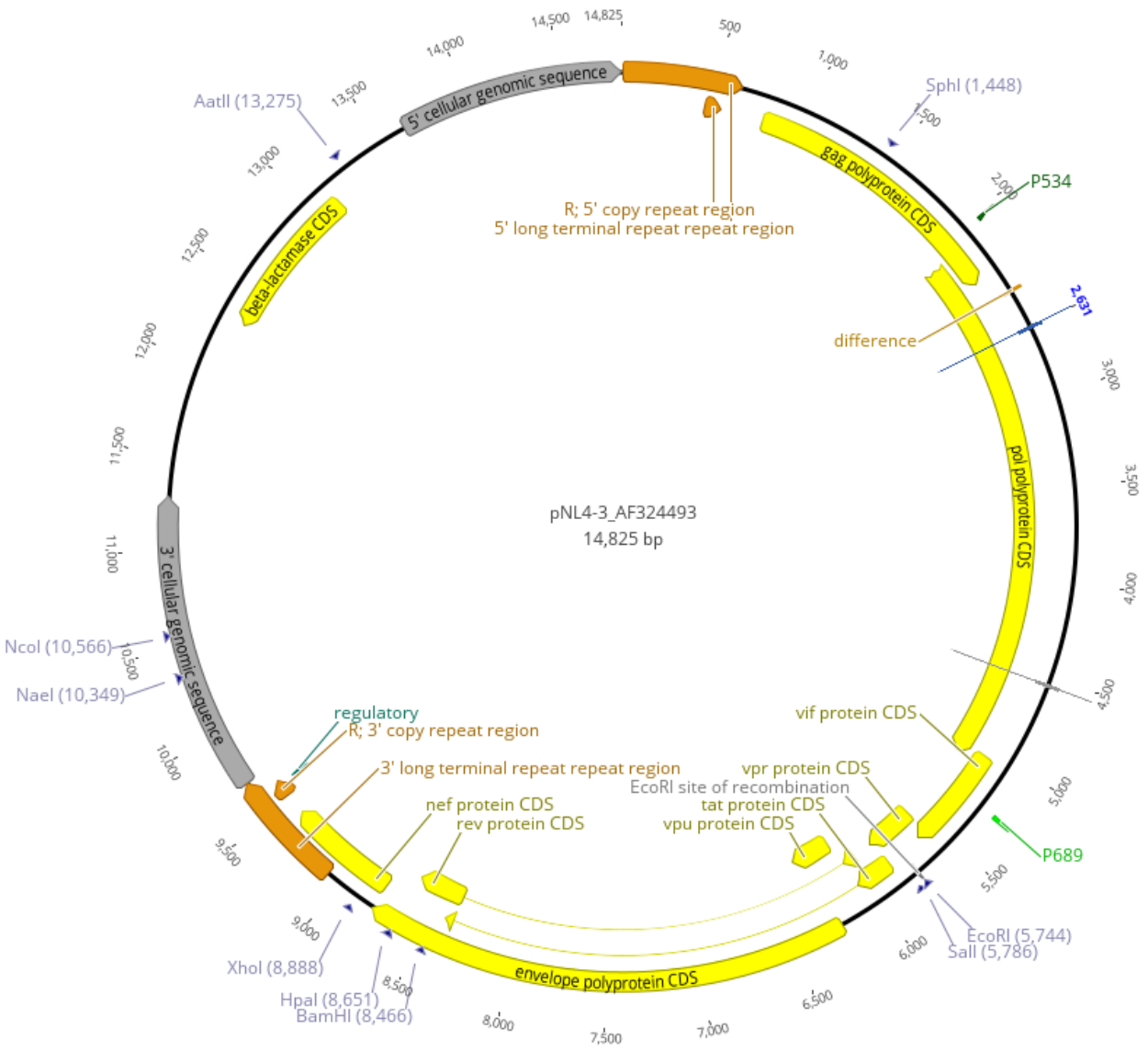

***Figure 12**: representation of pNL4-3 plasmid*

were blunt-ended cloned into pUC18 at the PvuII site after removal of polylinker sites. The pUC18 sequence holds the AmpR gene, conferring resistance to the antibiotic ampicillin. Upon transfection, this clone directed the production of infectious virus particles in a wide variety of cells. The NL4-3 virus uses CXCR4 as coreceptor and it has been used as reference wild-type virus in phenotypic assays.

3.2.2 pNL4-3ΔGAG-PR

To produce recombinant viruses carrying clinically derived HIV-1 GAG and PR coding regions, a modified version of pNL4-3 was employed in the transfection step. A region comprising the whole GAG and the protease coding sequence (coordinates 768-2602 based on the HIV-1 reference strain HXB2) was deleted from pNL4-3 through inverse PCR using amplification primers containing the recognition sequence for the restriction enzyme SacII. The inverse PCR fragment has been digested with SacII, then ligated to obtain the circular form of pNL4-3ΔGAG-PR, which could be propagated in suitable bacterial strains.

3.3 Antiviral drugs

The capsid inhibitor Lenacapavir (molecular formula: $C_{39}H_{31}ClF_{10}N_7O_5S_2$; molecular weight: 968.28 g/mol; MedChem Express) was supplied as a powder which was resuspended in dimethyl sulfoxide (DMSO). The stock solution was stored at -80°C and then diluted to prepare work solutions of 1nM, 10nM or 50nM in DMSO.

3.4 Generation of recombinant viruses harboring clinically derived GAG-PR region

3.4.1 Nucleic acid extraction and PCR amplification

For the amplification of the GAG-PR coding region, RNA from plasma samples was extracted using the EMAG automated extraction platform (BioMerieux) according to the manufacturer's protocol. The reverse transcription and first-round PCR were carried out at the same time using the SuperScript III One-Step RT-PCR with Platinum Taq High Fidelity (Invitrogen) including 10 µL of extract RNA, 25 µL of 2X Reaction Buffer, 20 U of Recombinant RNasin® Ribonuclease Inhibitor (Promega), 1 µL of SuperScript™ III RT with Platinum™ Taq High Fidelity Enzyme Mix, 0.1 µM of primer

P706 (5'-AACTAGGGAACCCACTGCTTAAG-3', HXB2 nucleotide coordinates 500-522) and LR51 (5'-TGTGGTATTCCTAATTGAACTTCCC-3', HXB2 2812-2836), and nuclease-free water to a final volume to 50 µL. The thermal cycling protocol included a reverse transcription step at 50°C for 30 minutes, followed by denaturation for 2 minutes at 94°C, and 35 cycles consisting of 56°C for 30 seconds, 68°C for 2 minutes and 30 seconds, and 94°C for 15 seconds, with a final step of 56°C for 1 minute and 68°C for 5 minutes. As template for a nested PCR were used 2 µL from the first-round PCR, which involved 0.5 U of Q5 Hot Start High-Fidelity DNA Polymerase (New England Biolabs), 6 µL of 5X Q5 Reaction Buffer, 83 µM of each dNTP, 0.1 µM of primer P207 (5'-GCCTCAATAAAGCTTGCCTTGA-3', HXB2 522-543) and P212 (5'-CTCCATTTAGTACTGTCYTTTTTYTTTAT-3', HXB2 2736-2764) with sterile nuclease-free water to a final volume of 30 µL. The thermal profile for nested PCR began with denaturation at 98°C for 30 seconds, followed by 35 cycles of 59°C for 30 seconds, 72°C for 1 minute and 30 seconds, 98°C for 10 seconds, with a final step of 59° for 1 minute and a 2-minute extension at 72°C. Both PCR reactions included a control tube with $2x10^6$ copies of pNL4-3, as a positive amplification control. 5 µL of the nested PCR products were loaded onto a 1.5% m/v Seakem agarose gel and electrophoresis was performed at 6 V/cm for 50 minutes. The presence of expected bands was verified under UV light using a Transilluminator after staining with GelRed dye (Biotium). Nested PCR was performed in triplicate to ensure an adequate amount of PCR product for the subsequent homologous recombination step with plasmid pNL4-3ΔGAG-PR.

3.4.2 Plasmid restriction and glycogen precipitation

For each recombinant virus harbouring clinically derived GAG-PR coding region, 10 µg of pNL4-3ΔGAG-PR were linearized through a restriction reaction consisting of 20 µL of rCutSmart Buffer 10X (New England Biolabs), 100 U of restriction enzyme SacII (New England Biolabs), 0.01 µM of a primer including the restriction site of SacII to enhance cleavage efficiency, and nuclease-free water to a final volume of 200 µL. Following an overnight incubation at 37°C, the restriction reaction was mixed with 75 µL of the GAG-PR region, amplified by nested PCR, from each plasma sample, 3 µL of glycogen 20 mg/µL, sodium acetate 244 mM and 600 µL of cold absolute Et-OH. The

solution was incubated for 20 minutes at -20°C, then equilibrated at room temperature before 15 minutes of centrifugation at 14,000 rpm for at 4°C. The pelleted DNA was washed twice with 70% Et-OH, then air-dried before the resuspension with 150 µL of nuclease-free water. Finally, the sample was stored at -20°C until the transfection with 293-LX.

3.4.3 293-LX cells transfection

293-LX cells transfection was performed following a calcium phosphate-based method to generate replication competent recombinant viruses through homologous recombination between linearized pNL4-3ΔGAG-PR and PCR amplicons. Twenty-four hours before the transfection, T25 flasks with 1-1.5 million of 293-LX cells were prepared for each transfection to reach 60%-70% confluence the day after. The day of transfection, purified DNA was mixed with 0.1X TE buffer (10 mM Tris, 1 mM EDTA, pH 8.0) to reach a final volume of 150 µL to which were added 16 µL of 2.5M $CaCl_2$. This solution was added to a previously prepared tube with 160 µL of 2X HPB (Hepes Phosphate Buffer: 50 mM Hepes, 0.3 M NaCl, 0.15 mM $Na_2HPO_4 \cdot 7H_2O$, pH 7.1) and incubated at room temperature for 30 minutes to allow the formation of $Ca_3(PO_4)$ crystals around the DNA. Meanwhile, 3 mL of fresh complete DMEM were added to each flask. The DNA solutions were gently added to each flask and incubated at 37°C with 5% CO_2 overnight, then culture medium was replaced with 5 mL of fresh DMEM, and the flasks were incubated in a Bio Safety Level 3 (BSL3) containment for 48 hours at 37°C with 5% CO_2. The supernatant from each transfection was harvested, centrifuged for 10 minutes at 300xg and stored in 2 mL aliquots at -80°C.

3.4.4 Viral expansion and titration

Recombinant viruses were used to infect MT-2 or U87-CXCR4 cells to increase the viral titer. Every 48 hours, infected cell cultures were monitored to check for the presence of multinucleated giant cells (syncytia) induced by HIV replication. Supernatants were mostly collected for 7-10 days post-infection, centrifuged at 300xg for 10 minutes to pellet the cells and debris, then cleared supernatants were stored in aliquots at -80°C.

Titration was performed on TZM-bl cells, which were firstly seeded in a 96-well culture plate at a density of 20,000 cells per well. The following day, the medium of each well was replaced with 150 µL of fresh medium, then 50 µL of each viral stock were aliquoted in the first well and progressively 4-fold diluted. After 48 hours of incubation at 37°C with 5% of CO_2, cells were washed twice with cold 1X Phosphate Buffered Saline (PBS, Sigma-Aldrich) buffer, then fixed with 40 µL of Fixation Buffer made of 0.25% glutaraldehyde pH 7.4 (Sigma-Aldrich) in PBS for 10 minutes at room temperature while gently rocking the plate. Cells were washed again with cold 1X PBS and then stained with 40 µL of freshly prepared Staining buffer (1 M $MgCl_2$, 0.5 M $K_4Fe(CN)_6 \cdot 3H_2O$, 0.5 M $K_3Fe(CN)_6$, 20 mg/mL X-Gal (Sigma-Aldrich) in dimethylformamide and 10X PBS for 2-20 hours at 37°C. Resulting dark blue-stained cells were counted with an inverted microscope and the $TCID_{50}$/mL was determined according to the formula:

$$\frac{TCID50}{mL} = number\ of\ blue\ cells * well\ fold\ dilution\ (where\ the\ cells\ were\ counted) * dilution\ factor\ to\ relate\ TCID50/50\ \mu L\ to\ 1\ mL$$

3.5 DNA Sanger sequencing

The Sanger sequencing protocol involved as first step the purification of PCR products with ExoSAP-IT Kit (Applied Biosystems), which included the preparation of a mixture made of 2 µL of ExoSAP-IT and 5 µL of sample. The mixture was then incubated for 15 minutes at 37° C and then inactivated for 15 minutes at 80°C. The sequencing reaction for the p24 coding region involved the preparation of a master mix consisting in 0.5 µL of Terminator Ready Reaction Mix 2X (NimaGen), 1.3 µL of BigDye Sequencing Buffer 5X (NimaGen), 0.32 µM of primer P1054 (5'-AGACAGGAWCAGARGAACTTARATCATTAT-3', HXB2 995-1024) and P1055 (5'-TTTTTYCTAGGGGCCCTGCAATTT-3', HXB2 1998-2021), 1-3 µL of purified PCR product and 4 µL of MilliQ water to a final volume of 10 µl. The thermal profile for this reaction included 96°C for 1 minute, 25 cycles of 96°C for 10 seconds, 50°C for 5 seconds and 60°C for 4 minutes. The sequencing reactions were then purified using the BigDye X-Terminator Kit (Applied Biosystems),

which consisted in the addition of 10 µL of X-Terminator Solution and 45 µL of SAM Solution in each well, then the plate was mixed in a 96-well microplate vortex at 3,000 rpm for 30 minutes followed by spinning for 3 minutes. Then, the plate with purified sequencing reactions was loaded into the 3130 XL Genetic Analyzer (Applied Biosystems) for the capillary electrophoresis sequencing. The resulting chromatograms were assembled and edited with the SeqMan v. 7.1.0 software (DNAStar).

3.6 Phenotypic susceptibility assay

Susceptibility to Lenacapavir was evaluated for 31 clinical samples on a TZM-bl cell-based luciferase assay. Cells were plated on a 96-well plate at a concentration of 15,000 cells/well and infected with HIV-1 with a multiplicity of infection (MOI) of 0.05 in presence of 5-fold dilutions of Lenacapavir (range 50 nM – 0.0256 pM). After 48 hours of incubation, 60 µL of Glo Lysis Buffer (Promega) were added to each well and the plates were incubated on an orbital shaker at 300 rpm at room temperature for 10 minutes to allow the cells lysis. 50 µL of the lysates were transferred to a white plate and mixed with 40 µL of Bright-Glo Luciferase Reagent (Promega), incubated for 2 minutes and then Relative Light Units (RLUs) in each well were measured through GloMax® Discover Microplate Reader luminometer (Promega). RLUs were elaborated with GraphPad Prism version 9.0.0 (GraphPad Software, Dotmatics) to calculate the half-maximal inhibitory concentration (IC_{50}) value of recombinant and wild-type viruses. Fold-change (FC) values were calculated as the ratio between the IC_{50} values of recombinant viruses and wild-type NL4-3 strain (**Figure 13**).

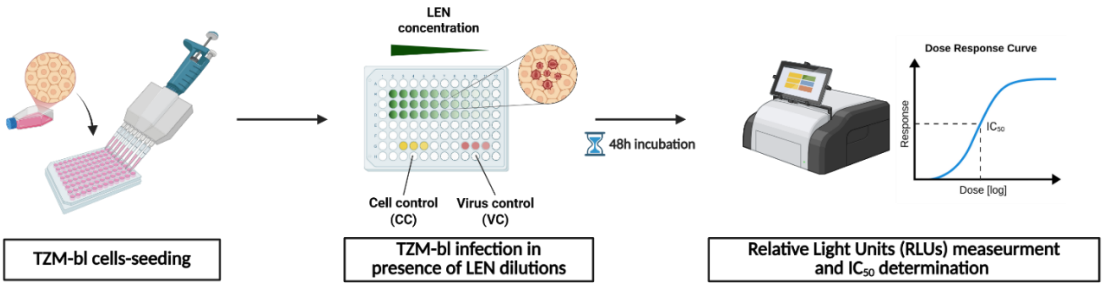

***Figure 13**: schematic representation of TZM-bl-based luciferase assay for Lenacapavir susceptibility determination (created in https://BioRender.com)*

3.7 *In vitro* resistance selection

3.7.1 *In vitro* resistance selection experiments

In vitro resistance selection experiments (IVRS) were performed by infecting MT-2 cells with each recombinant virus in presence of increasing concentration of Lenacapavir starting from 0.02 nM, which is approximately two times higher than the IC_{50} value of the NL4-3 virus. In presence of syncytia, the supernatant was harvested, centrifuged and partially used to infect a new culture of MT-2 cells in presence of a two-times higher concentration of Lenacapavir. The remaining supernatant was stored at -80°C and used for the extraction of viral RNA, amplification and sequencing of the p24 coding region to identify possible emerging mutations. IVRS were stopped if recombinant viruses were able to grow in presence of 2.56 nM of Lenacapavir or after approximately 100 days from the beginning of the experiments.

3.7.2 Viral RNA extraction, reverse transcription, amplification and DNA sequencing

For the sequencing of the p24 coding region from recombinant viruses, viral RNA was extracted using Quick-RNA Viral Kit (Zymo Research) following the manufacturer's instructions. Before the reverse transcription, 8 µL of extracted RNA were treated with the DNase I (Sigma-Aldrich) in a reaction including 1 µL of DNase Reaction Buffer 2X, 1 U DNase I and incubated for 15 minutes at room temperature, then mixed with 5 mM Stop Solution and incubated for 10 minutes at 70°C. DNAse-treated RNA was included in the reverse transcription reaction together with 10 µL of nuclease-free water, 6 µL of ImPromII 5X reaction buffer (Promega), dNTPs 170 µM, 50 ng of hexanucleotides (Promega), $MgCl_2$ 1.5 mM, 1 U of ImPromII Reverse Transcriptase (Promega), 20 U of rRNasin RNase Inhibitor (Promega) in a total volume of 30 µL. The reverse transcription reaction included 5 minutes at 25°C, 30 minutes at 37°C and 5 minutes at 80°C. Five microliters of cDNA were used as template for the amplification of the p24 coding region through a 40 cycles PCR including 1.5 U GoTaq polymerase (Promega), 6 µL of GoTaq 5X Buffer Green (Promega), dNTPs

30 µM, $MgCl_2$ 2.5 mM, 0.1 µM of each primer P1054 and P1055, and nuclease-free water to a final volume of 30 µL. The thermal cycling protocol included 94°C for 3 minutes, 40 cycles of 57°C for 30 seconds, 72°C for 1 minute, and 94°C for 30 seconds and then 57°C for 1 minute and 72°C for 3 minutes. PCR amplicons were sequenced as described in **paragraph 3.5**.

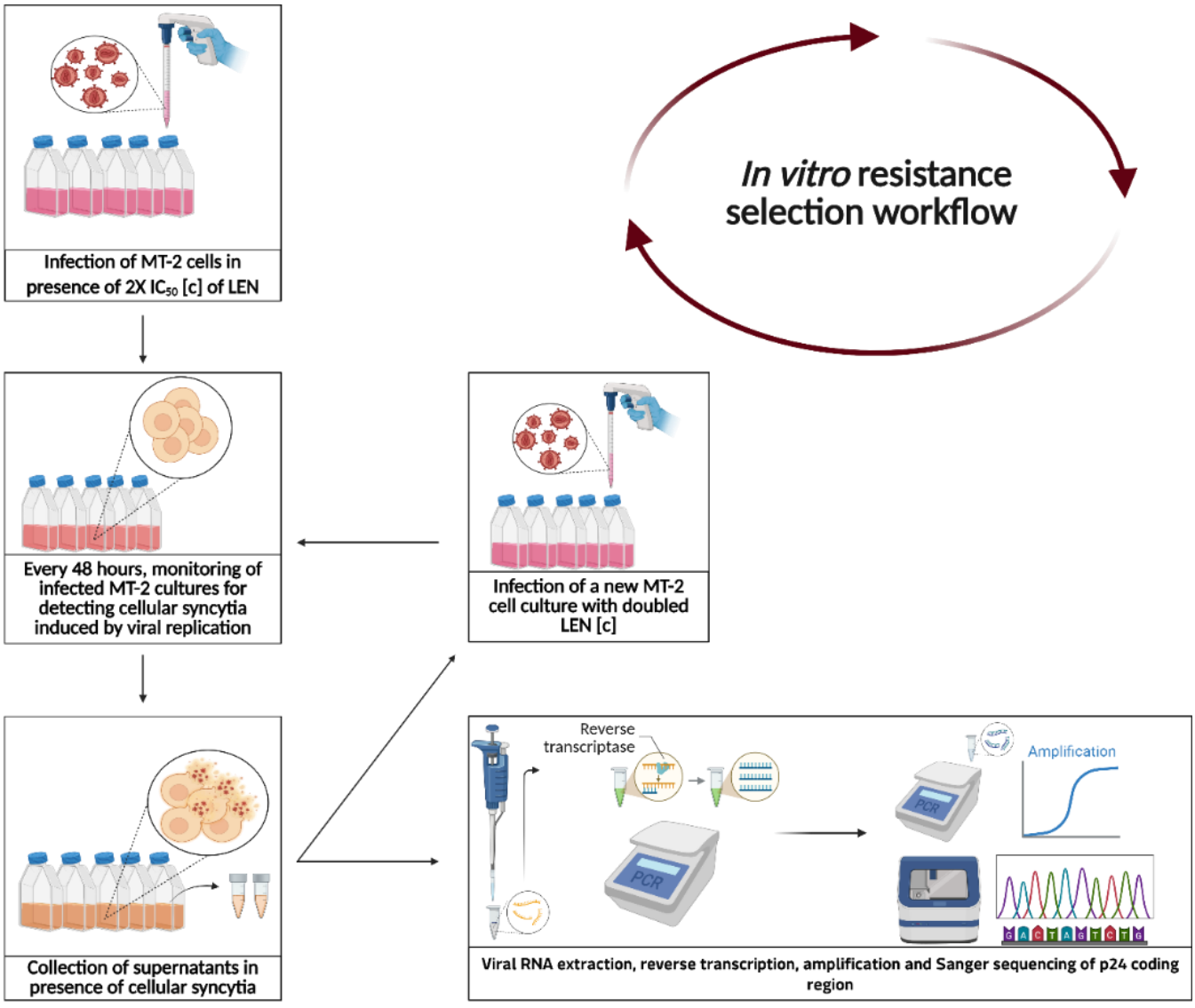

***Figure 14**: schematic representation of in vitro resistance selection workflow (created in https://BioRender.com)*

3.8 Cloning and mutagenesis

3.8.1 PCR amplification and purification

PCR amplicons for mutagenesis were generated as described in **paragraph 3.4.1** except for the nested PCR which was performed using the GoTaq® Long PCR Master Mix (Promega). Each reaction included 2 µL of cDNA, 12.4 µL of nuclease-free water, 15 µL of GoTaq Long Master Mix 2X (Promega) and 0.1 µM of primer P207 and P212. The thermal profile protocol included 2 minutes at 94°C, 35 cycles of 30 seconds at 48°C, 2 minutes and 30 seconds at 68°C and 30 seconds at 94°C, then 1 minute at 48°C and 10 minutes at 72°C. The amplified DNA was then purified using the QIAquick PCR Purification Kit (Qiagen), following the manufacturer's indications.

3.8.2 Ligation

The ligation step was performed using the pGEM®-T Easy Vector Systems by Promega. pGEM®-T Easy Vector is a linearized vector with a single 3'-terminal thymidine at both ends, which significantly enhances the ligation efficiency of PCR products by preventing the vector recircularization and providing a compatible overhang for PCR products. pGEM®-T Easy Vector are supplied with 2X Rapid Ligation Buffer whose use allows the incubation of the ligation reaction for 1 hour at room temperature, even if an extended incubation period may increase the number of bacterial colonies after transformation. Indeed, an overnight incubation at 4°C maximizes the number of transformants. Besides the 2X Rapid Ligation Buffer, the reaction components involved 50 ng of pGEM®-T Easy Vector, ~15 ng of PCR product and 3 Weiss units of T4 DNA ligase to reach a final reaction volume of 10 µL. The molar ratio between vector and insert used was 3:1. Following overnight incubation at 4°C, the ligation reaction was ready for the transformation into competent bacterial cells.

3.8.3 Bacterial strains and transformation

The cells used for transformation were DH10B, chemically competent E. coli cells [genotype: F-endA1 recA1 galE15 galK16 nupGrpsL ΔlacX74 Φ80lacZΔM15 araD139 Δ(ara,leu)7697 mcrA Δ(mrr-hsdRMS-mcrBC) λ-] purchased from Invitrogen. The protocol suggested by Eppendorf (Hamburg, Germany) to obtain electro-competent cells was followed and required the mixing of 1-10 ng of DNA with an aliquot of competent cells. Subsequently, the mixture was transferred in a previously cooled sterile cuvette, then electroporated with the use of the Eppendorf Multiporator instrument at 1700 V for 5 ms. Immediately following the electroporation, 500 µL of Super Optimal Broth with Catabolite Repression (SOC) medium (950 mL H_2O, 20 g of tryptone, 5 g of yeast extract, 0.5 g of NaCl, 2.5 mM KCl, 0.2 mM $MgCl_2$ and 20 mM of glucose; Thermo Fisher Scientific) were added to the cells that were consequently incubated for 1 hour at 37°C in an orbital shaker. Later, the cells were plated on Luria Bertani Agar (LBA) plates (1% tryptone, 0.5% yeast extract, 1% NaCl, 15 g/l agar; Thermo Fisher Scientific) in presence of 100 µg/mL of Ampicillin (Sigma-Aldrich) and incubated at 37°C overnight.

3.8.4 Selection of positive colonies

The presence of colonies harboring the plasmid with the desired PCR fragment were detected through a colony PCR where a small amount of each colony was added to a reaction mix including 19.9 µL of nuclease-free water, 6 µL of GoTaq 5X Buffer Green (Promega), dNTPs 30 µM, 1.5 U GoTaq polymerase (Promega), $MgCl_2$ 2.5 mM and 0.1 µM of primer P1054 and P1055 in a final volume of 30 µL. The thermal profile consisted of 10 minutes at 94°C, 35 cycles of 55°C for 30 seconds, 72°C for 1 minute and 94°C for 30 seconds, then 1 minute at 55°C and 72°C for 2 minutes. Amplicons were sequenced as described in **paragraph 3.5**, then colonies with the expected PCR fragment were inoculated in LB solution (1% tryptone, 0.5% yeast extract, 1% NaCl) for an overnight incubation at 37°C and 200 rpm horizontal shaking. The plasmid DNA was extracted from each bacterial culture with the QIAprep Spin Miniprep Kit (Qiagen) and then quantified with the Qubit 4 Fluorometer (Invitrogen) following the manufacturer's instructions.

3.8.5 Site-directed mutagenesis

Site-directed mutagenesis was performed using the QuickChange MultiSite-Directed Mutagenesis Kit (Agilent) to modify specific nucleotides from recombinant virus sequences, resulting in the introduction or deletion of specific patterns of resistance mutations. The mutagenesis procedure followed a three-step protocol which involved, as first step, a thermal cycling reaction for mutant strand synthesis. This reaction included 1X QuickChange Multi reaction buffer, 50 ng of double-stranded DNA template, 100 ng of mutagenic primers including the desired mutation designed by the web-based Agilent tool, 1 µL of dNTPs mix, 1 µL of QuickChange Multi enzyme blend and nuclease-free water to a final volume of 25 µL. The cycling parameters consisted of 1 minute at 95°C and 30 cycles of 95°C for 1 minute, 55°C for 1 minute and 65°C for 8 minutes. The second step consisted of the digestion of each mutagenesis reaction with Dpn I (10 U/µL), a restriction endonuclease specific for the digestion of methylated and hemimethylated parental DNA. Dpn I reaction was carried out for 1 hour at 37°C to remove the non-mutated DNA templates. In the third step, the DpnI-treated mutagenesis reaction was transformed into DH10B ultracompetent cells for cloning and subsequent DNA sequencing to verify the presence of the desired mutations (see **paragraph 4.4**).

3.8.6 Susceptibility to Lenacapavir of site-directed mutants

Recombinant viruses harboring different patterns of mutations derived from site-directed mutagenesis were generated as described in **paragraph 3.8.5**. Susceptibility to Lenacapavir was measured as described in **paragraph 3.6**.

4 RESULTS

4.1 Study characteristics and population

This study analyzed the susceptibility and the genetic barrier to resistance to Lenacapavir, a novel first-in-class HIV-1 capsid inhibitor, using 31 plasma samples collected from PWH, 20 from treatment-naïve (TN) and 11 from heavily treatment-experienced (HTE) individuals. Samples from HTE PWH were obtained from the Italian PRESTIGIO registry.

4.2 Baseline phenotypic susceptibility to Lenacapavir

Recombinant viruses based on the wild-type NL4-3 strain bearing clinically derived GAG-PR region were successfully generated from all 31 plasma samples. For each recombinant virus, IC_{50} was calculated and expressed as FC value, according to **paragraph 3.6** (**Table 3**). Among recombinant viruses, GAG-PR belonged to subtype B in 12 cases and non-B in 19 cases (1 each of A1, G, URF D/B and CRF40_BF, 2 each of C, CRF01_AE and CRF06_cpx and 3 each of F1, D and CRF02_AG) (**Figure 15**).

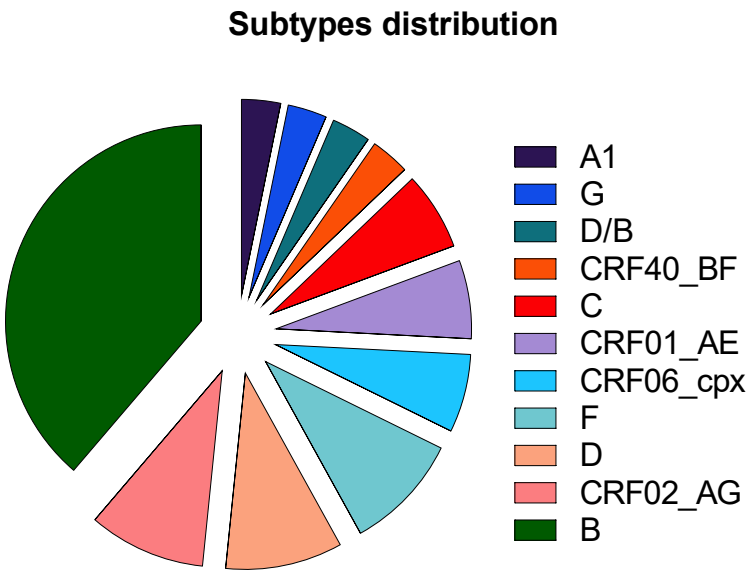

***Figure 15**: subtypes prevalence distribution among all the 31 clinically derived viruses*

	Treatment Status	Subtype	IC_{50} ± SD (pM)	Fold-Change
WT NL4-3		B	26 ± 20	
155584	TN	D	17 ± 4	0.6
155590	TN	CRF06_cpx	19 ± 5.1	0.7
156034	TN	F1	79 ± 4	3.0
156083	TN	C	43 ± 8	1.6
156338	TN	G	79 ± 54	3.0
156439	TN	CRF02_AG	28 ± 6	1.0
156850	TN	B	5 ± 1	0.2
153181	HTE	B	16 ± 5	0.6
153175	HTE	B	6 ± 2	0.2
156436	TN	CRF02_AG	14 ± 3	0.5
156004	TN	A1	47 ± 32	1.8
156890	HTE	D	42 ± 12	1.6
156891	HTE	CRF02_AG	62 ± 1	2.3
156894	HTE	F	42 ± 35	1.6
153233	HTE	B	7 ± 5	0.3
153230	HTE	B	37 ± 16	1.4
153178	HTE	B	6 ± 1	0.2
153170	HTE	B	15 ± 4	0.6
151986	HTE	B	23 ± 2	0.9
155403	TN	CRF01_AE	13 ± 5	0.5
156203	TN	C	347 ± 14	13.1
155816	TN	CRF01_AE	84 ± 16	3.2
156239	TN	A6	24 ± 6	0.9
156872	TN	B	33 ± 9	1.2
156868	TN	B	65 ± 26	2.4
156027	TN	F1	59 ± 22	2.2
156892	HTE	CRF40_BF	310 ± 71	11.7
156875	TN	B	149 ± 44	5.6
156873	TN	B	85 ± 8	3.2
155588	TN	D	58 ± 21	2.2
155591	TN	CRF06_cpx	202 ± 53	7.7

***Table 3**: phenotypic susceptibility to Lenacapavir expressed as fold-change with respect to NL4-3 strain. TN = treatment-naïve; HTE = heavily-treatment experienced; IC_{50} = half-maximal inhibitory concentration; SD = standard deviation*

Viruses with B and non-B subtypes showed a comparable median (IQR) baseline FC value of 0.8 (0.2 - 2.2) and 1.8 (0.9 - 3.0), respectively (p = 0.051, Mann-Whitney test) (**Figure 16B**). Similarly, HTE and TN values (**Figure 16A**), had a comparable median (IQR) baseline FC value of 0.9 (0.3 - 1.6) and 2.0 (0.8 - 3.2), respectively (p = 0.101, Mann-Whitney test).

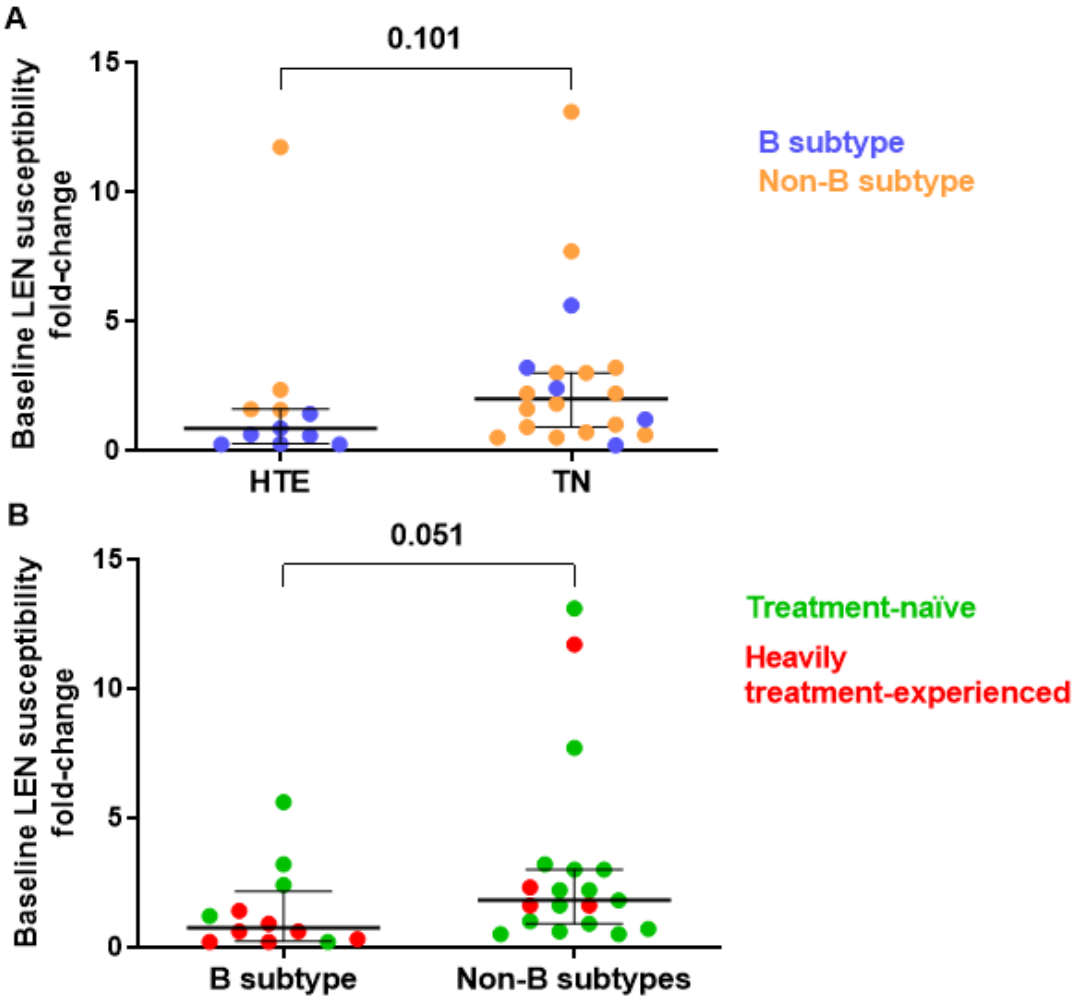

***Figure 16**: comparison of baseline fold-change Lenacapavir susceptibility of HTE vs. TN (**A**) and B vs. non-B subtypes (**B**) clinically derived viruses. HTE = heavily-treatment experienced; TN = treatment-naïve*

4.3 *In vitro* resistance selection results

A Kaplan-Meier survival analysis was performed to assess and compare the timing of viral breakthrough, measured as the number of days from the start of the experiments, at LEN

concentrations of 0.32 nM and 2.56 nM, corresponding to approximately 10-fold and 100-fold the IC_{50} of the NL4-3 strain. While the time of viral breakthrough between viruses harboring GAG-PR sequences from HTE and TN PWH was comparable at both 10X and 100X LEN (p = 0.284 and p = 0.131, respectively) (**Figure 17B**), viruses with subtype B GAG-PR coding region showed a lower time for viral breakthrough with respect to non-B subtypes at both 10X and 100X LEN (p = 0.047 and p = 0.026, respectively) (**Figure 17A**).

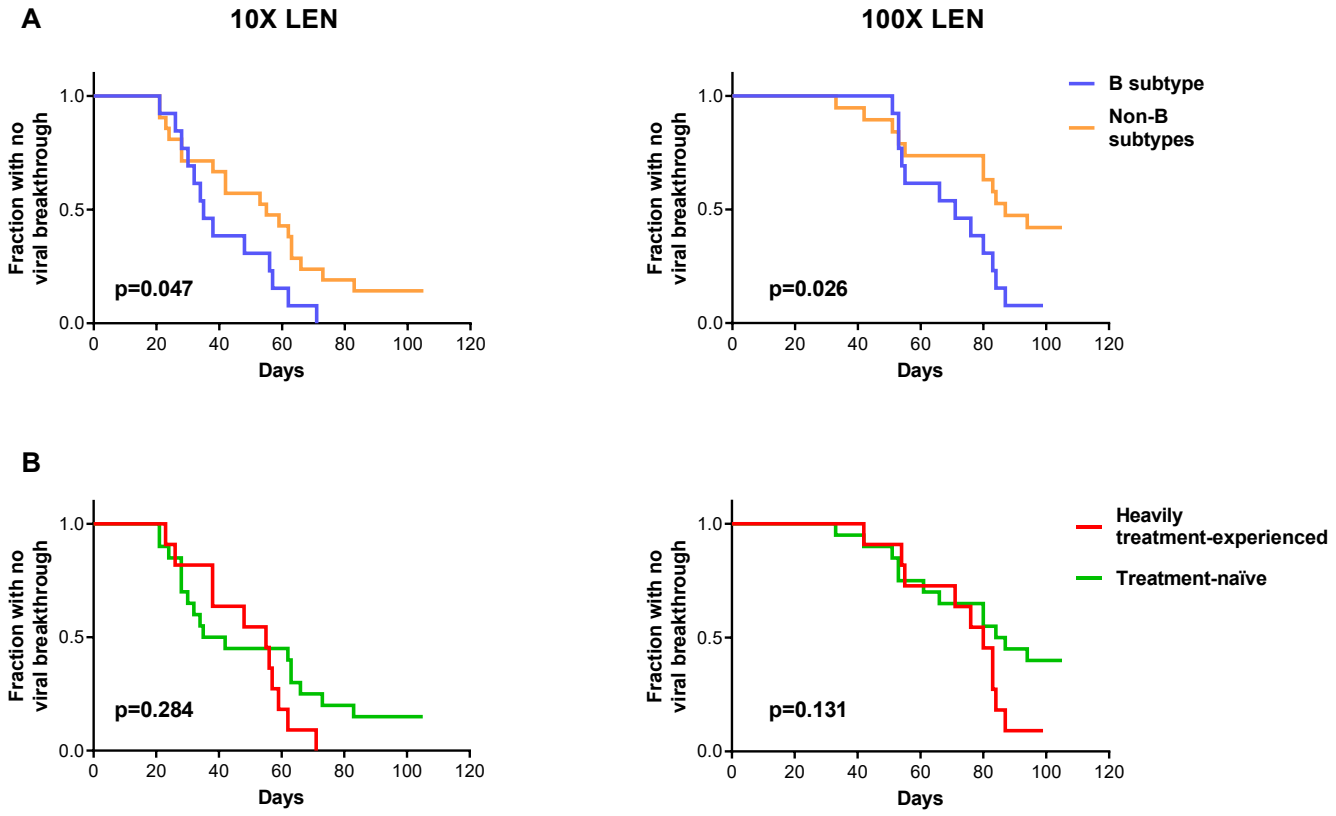

***Figure 17**: Kaplan-Meier survival analysis of the time of viral breakthrough for B and non-B subtypes (**A**) and therapy-naïve and heavily treatment-experienced (**B**) clinically derived viruses at approximately 10X and 100 X Lenacapavir concentration*

In vitro resistance selection experiments were performed in MT-2 cells for a period of no longer than 105 days. The results of these experiments revealed the emergence of mutations known to be associated with Lenacapavir resistance in almost all recombinant viruses and in the culture with NL4-3 virus. Indeed, mutations were identified in 27 out of 32 cell cultures, the mutational patterns were Q67H/R/K+N74D in seven cases, Q67H/K+T107N/S in six cases, N74D in five cases,

N74D+T107N/D in three cases, while Q67H+K70R+T107N, Q67H+K70R and Q67H in two cases. In five cases where cultures were stopped, no emerging mutations were observed (**Table 4**).

The distribution of emerging patterns of mutations was comparable between subtypes B and non-B, while cases without emerging mutations were observed in non-B subtypes only (**Figure 18**). In addition, three non-polymorphic amino acids substitutions (e.g., amino acid variants with a prevalence <1% with respect to circulating isolates, source Los Alamos National HIV-1 database, https://www.hiv.lanl.gov/) such as F169L, V86M and E213D emerged in association with mutations Q67H+T107TN, Q67H+K70R and Q67H+T107N, respectively. Other non-polymorphic substitutions detected as mixed viral populations at some LEN concentrations were D71DN, I91IT, S102SN, R132RK, R143RK, while two uncommon amino acid substitutions at LEN resistance position were A107D in sample 153170 and Q67R in sample 156891.

Regarding the RAMs emergence between B and non-B subtypes groups along the IVRS experiments, no significant differences were observed except for Q67QH/H mutations (83.33% B vs. 36.84% non-B, p = 0.025, Fisher's exact test) (**Figure 19**) observed in the 31 clinically-derived HIV-1 isolates.

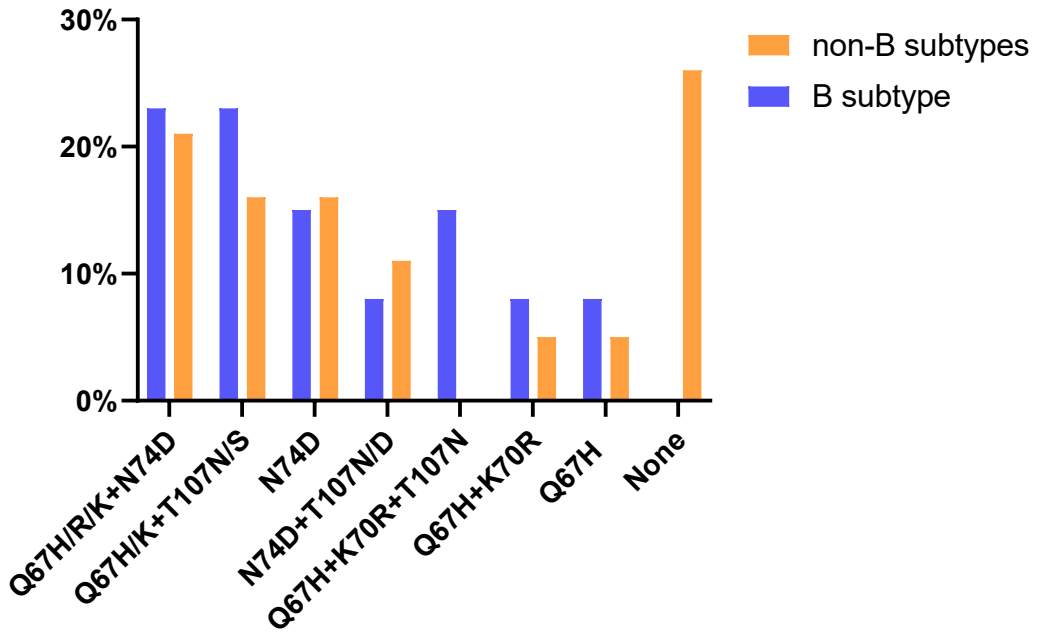

***Figure 18**: distribution of selected HIV-1 mutations associated with Lenacapavir resistance between B and non-B subtypes*

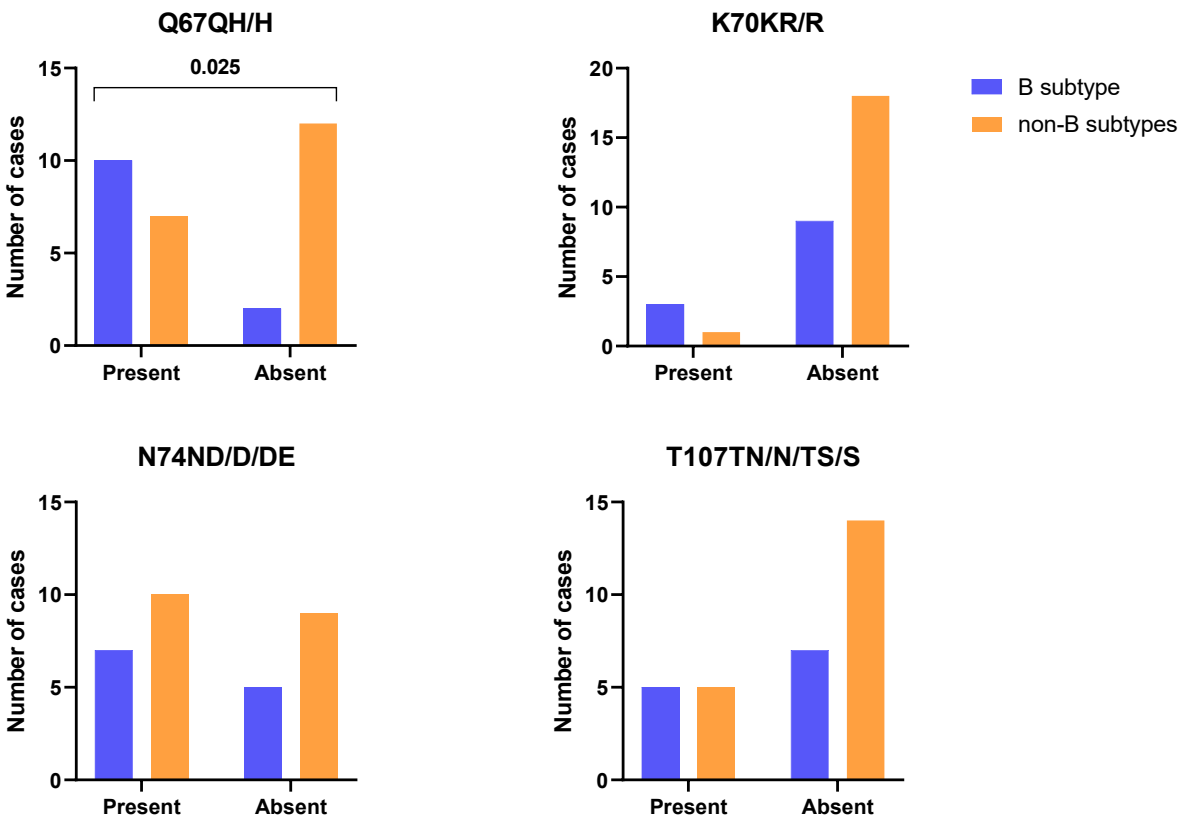

***Figure 19**: overall representation of resistance-associated mutations' detection between B and non-B subtypes among all Lenacapavir concentrations tested in IVRS experiments*

Sample	Lenacapavir [c] nM						
	0.04	0.08	0.16	0.32	0.64	1.28	2.56
WT NL4-3				Q67QH, N74ND, **E213D**	Q67QH, N74D, **E213D**	Q67QH, N74D, **E213D**	Q67H, T107N, **E213D**
155584		M96L	M96L	M96L	Stopped at 0.64 nM after 105 days		
155590					Q67H	Sanger sequencing failure due to mixed viral population	S41ST, L56LV, Q67QL, N74D
156034					Stopped at 0.64 nM after 105 days		
156083				N74DE	N74D	N74D	N74D
156338				Q67H	Q67H, **F169L**	Q67H, T107TN, **F169L**	Q67H, T107N, **F169L**
156439						N74D, V83VI, H87HQ	N74D, V83VI, H87HQ, R154RK
156850					N74D	Q67H, N74D	Q67H, N74D
153181					Q67QH, N74ND	Q67QH, N74ND, T107TN	Q67H, N74D, R132RK
153175			Q67H	Q67H	Q67H, K70R, **V86M**	Q67H, K70R, **V86M**	S41SA, Q67H, K70R, **V86M**
156436					Q67QH, N74ND, T107S, I124IV	N74D, T107S, I124V	T58TI, Q67QK, T107S, I124V
156004				N74D, T107TN	N74D, T107TN	N74D	Stopped at 2.56 nM after 99 days
156890			N74ND, T107TN	N74ND, T107TN	N74D, T107TN	N74D, T107TN	N74D, T107N
156891				N74D, **I91IT**	N74D	N74D, **I91IT**	N74D, Q67R
156894		154RK	N74D, K154RK	N74D, K154R	N74D, K154R	T58TI, N74D, D71DN, K154R	T58TI, Q67QK, D71DN, N74D, K154R
153233		Q67H	Q67H	Q67H, T107N	Q67H, T107N	Q67H, T107N	Q67H, K70KR, T107N
153230			N74ND	N74D	N74D	N74D, H87Q	Q67H, N74D
153178			N74D	N74D	N74D	Stopped at 1.28 nM after 99 days	
153170		**107A**	**A107D**	**A107D**	**A107D**	N74D, **A107D**	N74D, **A107D**
151986			Q67H, T107TN	Q67H, T107N	Q67H, T107N	Q67H, T107N	Q67H, K70R, T107N
155403		Q67H	Q67H	Q67H	Q67H	Q67H, T107TN, **S102SN**	Q67H, T107N
156203	**A88T**		**R143RK**, T200N	Stopped at 0.32 nM after 100 days			
155816		Stopped at 0.08 nM after 84 days					
156239		M10I, V124I	M10I	Stopped at 0.32 nM after 81 days			
156872			Q67H	Q67H	Q67H, N74ND, T107TN	Q67H, T107N	Q67H, T107N
156868	I15L, Q67QH	I15L, Q67QH	T107TN	N74ND, T107TN	N74D, H87Q	A14T, N74D, H87Q	A14T, N74D, H87Q, **L172LI**
156027		I15L, Q67QH	I15L, Q67H	I15L, S41SA, Q67H	I15L, S41SA, Q67H	I15L, S41A, Q67H, K70R	I15L, S41A, Q67H, K70R
156892					N74D	N74D	N74D
156875			Q67H	Q67H	Q67H, T107TN	Q67H, T107N	Q67H, T107N
156873		H87Q	Q67H, H87Q	Q67H, H87Q	Q67H, H87Q	Q67H, E71D, H87Q	Q67H, E71D, H87Q
155588		V86VM	Q67H, **V86M**	Q67H, **V86M**	Q67H, **V86M**	Q67H	Stopped at 2.56 nM after 101 days
155591			A14S, H87Q	A14S, H87Q	A14S, Q67QH, H87Q	N74D, H87HQ	Q67QH, N74ND

***Table 4**: Emerging mutations at specific Lenacapavir concentrations during in vitro resistance selection experiments. Mutations in bold indicate emerging non-polymorphic substitutions not previously described in literature. Empty boxes indicate the absence of emerging mutations with respect to the baseline sequences*

Overall, at each LEN concentration tested in IVRS experiments, days of viral breakthrough observed were similar between B and non-B subgroups, indicating a common time of RAMs emergence. Moreover, the presence of the Q67H and T107N mutations among all HIV-1 isolates at 2.56 nM concentration (46.2% and 30.8%, respectively) seemed to be the principal drivers in conferring LEN-resistance (**Figure 20**).

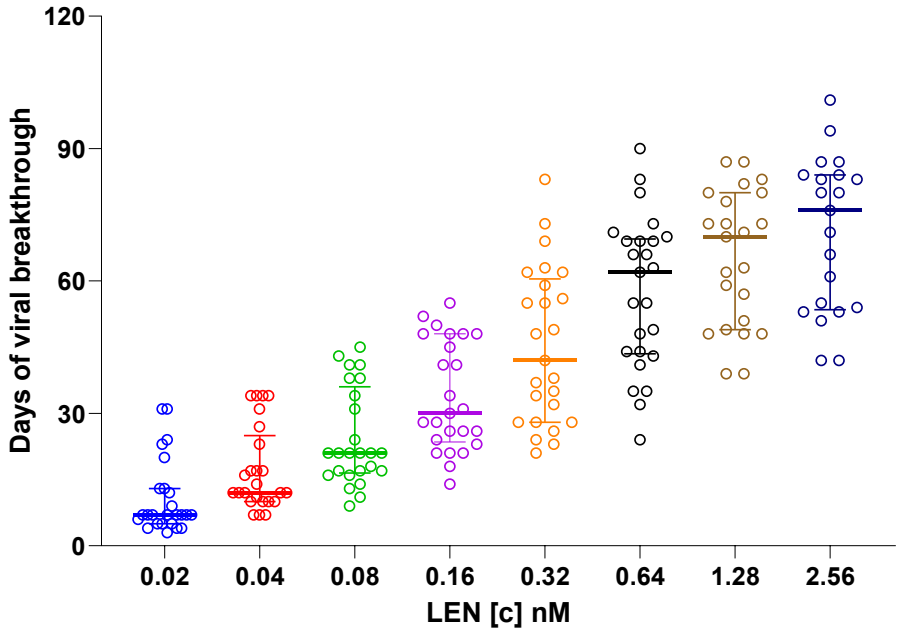

	Lenacapavir [c] nM							
Resistance Associated Mutations (RAMs)	**0,02**	**0,04**	**0,08**	**0,16**	**0,32**	**0,64**	**1,28**	**2,56**
Q67QH		3,9%	7,7%		3,9%	11,5%	7,7%	
Q67H			7,7%	34,6%	38,5%	42,3%	42.3%	46,2%
K70KR								3,9%
K70R						3,9%	7,7%	1,6%
N74ND				7,7%	11,5%	11,5%		
N74D				7,7%				
N74DE					3,9%			
T107TN				11,5%	11,5%	15.4%	15.4%	
T107N					7,7%	3,9%		30,8%
T107TS								3,9%
T107S							3,9%	

***Figure 20**: representation of days of viral breakthrough between B and non-B subtypes along all the Lenacapavir concentrations tested in IVRS experiments. In the table below, overall frequences of RAMs emergence at each concentration are shown.*

4.4 Characterization of non-polymorphic substitutions impact on Lenacapavir susceptibility

Next, we decided to evaluate the impact of non-polymorphic substitutions Q67R, V86M, A107D, F169L, and E213D together with concomitantly emerging mutations using site-directed mutagenesis for creating different patterns of mutations in the same genetic context of recombinant viruses. For this purpose, specific mutagenesis primers were designed to introduce or remove selected mutations (**Table 5**). This approach aimed to generate a set of variants for evaluating how different mutations impact LEN susceptibility. Regarding the non-polymorphic substitution A107D, mutagenesis was not performed as it was already present in the viral supernatant, and thus it was compared directly with other supernatants. On the other hand, the investigation of E213D is still ongoing, as it has not been successfully obtained through mutagenesis.

Samples	Starting mutations	Primers' sequence and coordinates	Resulting Mutations
156891	N74D	**P1096**: 5'-GAAGTGACATAGCAGGAAATACTAGTACCCTGCAGG-3'; HXB2: 1487-1522 **P1097**: 5'-AGAGATTATGTAGATAGGTTCTTTAAAACCTTGAGAGCTGAGC-3'; HXB2: 1669-1711	N74D + **Q67R**
155588	Q67H + **V86M**	**P1108**: 5'-GGGACATCAAGCAGCTATGCAGATGTTAAAAGAAACCATCAAT-3'; HXB2: 1365-1407 **P1109**: 5'-TGGGACAGGATGCATCCAGTGCAAGCAGGG-3'; HXB2: 1423-1452	**V86M**
156338	Q67H + **F169L**	**P1095**: 5'-GGCATCAAGCAGCTATGCAAATGCTAAAGGATACTATCA-3'; HXB2: 1367- 1405	**F169L**

***Table 5**: sequences and coordinates of mutagenic primers for mutants' generation.*

To date, only some mutant recombinant viruses harboring target RAMs with or without non-polymorphic substitutions were obtained, due to problems of viral expansion possibly related to low replication capacity. Results of susceptibility to LEN of these recombinant viruses were expressed as FC values with respect to their baseline LEN IC_{50} in **Table 6**.

Curiously, the S102N in combination with the Q67H RAM seemed reduce LEN susceptibility by ~7-fold compared to Q67H alone. Similarly, non-polymorphic substitutions S41A and V86M reduce LEN susceptibility only when in combination with Q67H and/or K70R RAMs.

Samples	Mutations selected	IC_{50} ± SD nM	Fold-Change
155403	Q67H	1.289 ± 1.639	99.1
	Q67H+S102N	8.300 ± 0.566	638.5
153175	S41A+V86M	0.004 ± 0.001	0.7
	Q67H+K70R+V86M	4.375 ± 0.757	729.2
	S41A+Q67H+K70R+V86M	11.375 ± 2.949	1895.8
155588	V86M	0.007 ± 0.001	0.1
	Q67H+V86M	0.710 ± 0.141	12.2

***Table 6**: evaluation of Lenacapavir susceptibility of mutant viruses harboring RAMs and/or non-polymorphic substitutions. Fold-Change values indicate Lenacapavir susceptibility differences with respect to the baseline one. IC_{50} = half-maximal inhibitory concentration; SD = standard deviation*

5 DISCUSSION

HIV-1 management remains a major global health challenge, despite substantial improvements in antiretroviral therapy, diagnosis and prevention. Over the past decades, many highly effective drugs have been developed and licensed, enabling durable viral suppression, reducing adverse events and improving the quality of life of PWH, which in turn helps reducing stigma and the psychological burden of living with the disease.

Currently first-line regimens typically combine two or three drugs from different classes, aiming to target multiple steps of viral replication cycle and lower the risk of the emergence of resistance. Despite their effectiveness, earlier regimens generally lacked the potency, tolerability and the convenience of dosing frequency that is common for current regimens. Consequently, PWH with long treatment history, particularly those with suboptimal adherence when exposed to earlier regimens, may have accumulated mutations causing MDR, thus limiting treatment options and complicating clinical management. This justify the need for new drugs with alternative mechanisms of action, better safety profiles and long-acting formulations. One remarkable example of this scenario is the long-acting injectable regimen comprising the INSTI cabotegravir and the NNRTI rilpivirine, administered every one or two months in PWH with suppressed viral load for at least six months and without prior virological failure with agents belonging to the NNRTI or INSTI class (Nachega *et al.*, 2023). Despite the high treatment satisfaction and reassuring low risk of virological failure reported in clinical trials, the frequent selection of emergent resistance at failure has shown to cause extensive intraclass resistance, suggesting a suboptimal genetic barrier to resistance. Strategies for mitigating this risk include the closer monitoring of viral load and the genotype on proviral DNA before the start of the therapy, aiming to exclude the presence of NNRTI resistance mutations (Ripamonti, Borghetti and Zazzi, 2024).

Another example is represented by lenacapavir, the first-in-class capsid inhibitor approved for the treatment of MDR HIV-1 infection with a twice-yearly administration, acting at picomolar concentration against multiple viral subtypes and throughout different stages of viral replication (Link *et al.*, 2020; Hitchcock *et al.*, 2024; Margot *et al.*, 2025). Due to its unique mechanism of

action, lenacapavir has no known cross-resistance with other existing drug classes (Link et al., 2020).

More recently, phase 2 and phase 3 PURPOSE -1 and -2 clinical studies demonstrated the strong efficacy of lenacapavir administered twice-yearly as PrEP (Bekker *et al.*, 2024; Kelley *et al.*, 2025), resulting in a 100% and 96% reduction of risk of HIV infection, respectively, when compared with the daily oral emtricitabine/tenofovir formulation currently recommended for PrEP.

The development of lenacapavir represent a major advancement in the antiretroviral therapy, since it is the most potent (antiviral activity in the sub-nanomolar range *in vitro*) and the longest-acting dosing among antiretrovirals developed so far. However, *in vitro* testing and clinical trials evidenced the rapid and frequent selection of resistance-associated mutations which confer decreased susceptibility to lenacapavir (Margot *et al.*, 2021; Neverette *et al.*, 2025), particularly when used as functional monotherapy in PWH with no remaining fully active drugs available, suggesting low genetic barrier to resistance (Segal-Maurer *et al.*, 2022).

Since most data on the selection of resistance have been obtained from subtype B isolates, this study was designed to comprehensively characterize the *in vitro* genetic barrier to resistance to lenacapavir in HIV-1 B and non-B subtypes isolated from both TN and HTE PWH.

Recombinant viruses harboring clinically derived GAG-PR region from individuals with B and non-B subtypes, including both TN and HTE PWH, showed comparable susceptibility to lenacapavir levels regardless of subtype (B vs. non-B) and treatment history (TN vs. HTE), indicating that natural genetic variability and prolonged exposure to antiviral drugs may have no impact on the activity of lenacapavir.

In vitro resistance selection analysis showed that exposure to sub- or fully inhibitory lenacapavir concentrations resulted in the selection of resistance mutation in most infected cultures, confirming the low-level genetic barrier to resistance of lenacapavir. The main finding was that RAMs were selected at known amino acid positions in both B and non-B subtypes, indicating that the genetic variability of the p24 capsid protein coding region doesn't affect lenacapavir antiviral activity. Interestingly, overall time to viral breakthrough of B subtype-based viruses was lower than non-B ones, with the Q67QH/H mutation more prevalent in B than non-B subtypes, suggesting a possible lower time to RAMs development and higher replicative capacity in B than non-B subtypes.

During IVRS experiments, we also detected some amino acidic substitutions within the p24 capsid protein region, maybe not directly involved in lenacapavir resistance but possibly acting as compensatory mutations. Indeed, we found both polymorphic and non-polymorphic substitutions that have emerged in few cases together with known RAMs, suggesting a possible role in enhancing viral fitness and contributing to decrease lenacapavir susceptibility as demonstrated by mutagenesis experiments.

Our study has some limitations. The time to viral breakthrough and the selection of resistance mutations might have been affected by the reduced low replication capacity related to the chimeric nature of recombinant viruses. Indeed, the clinically derived sequences encompassing the whole GAG and the PR coding region were included in the genetic background of the NL4-3 genome, which is a subtype B strain. Although all the recombinant viruses have shown to propagate in cell culture, we may not exclude that suboptimal interactions between viral proteins from the clinically derived sequences, particularly those from non-B subtypes, and those from the NL4-3 strain may have influenced the outcome of the experiments. A possible alternative is represented by the use of primary isolates, although the difficulty for the direct isolation of isolates from plasma that can be propagated in cell lines, or preferably using primary $CD4^+$ T cells, make this solution not suitable.

In conclusion, our study reinforces that the antiviral potency of Lenacapavir is not affected by the natural variability or previous exposure to antiviral treatments, but also confirms the low genetic barrier to resistance. Our data underscores the clinical importance of constructing an optimized background regimen that includes, whenever possible, at least one fully active antiviral drug in combination with lenacapavir, in order to maintain viral suppression and minimize the risk of resistance development.

6 References

95-95-95 targets - UNAIDS (2025). Available at: https://doi.org/https://www.unaids.org/en/resources/documents/2024/progress-towards-95-95-95.

Arts, E.J. and Hazuda, D.J. (2012) "HIV-1 antiretroviral drug therapy," *Cold Spring Harbor Perspectives in Medicine*, 2(4). Available at: https://doi.org/10.1101/cshperspect.a007161.

Aulicino, P.C. *et al.* (2024) "Variable antiviral activity of islatravir against M184I/V mutant HIV-1 selected during antiretroviral therapy.," *The Journal of antimicrobial chemotherapy*, 79(2), pp. 370–374. Available at: https://doi.org/10.1093/jac/dkad390.

Ayinde, D. *et al.* (2010) *Limelight on two HIV/SIV accessory proteins in macrophage infection: Is Vpx overshadowing Vpr?* Available at: http://www.retrovirology.com/content/7/1/35.

Barré-Sinoussi, F. *et al.* (1983) *Isolation of a T-Lymphotropic Retrovirus from a Patient at Risk for Acquired Immune Deficiency Syndrome (AIDS)*, *Montagnier Source: Science, New Series*.

Bekker, L.-G. *et al.* (2024) "Twice-Yearly Lenacapavir or Daily F/TAF for HIV Prevention in Cisgender Women," *New England Journal of Medicine*, 391(13), pp. 1179–1192. Available at: https://doi.org/10.1056/nejmoa2407001.

Berger, E.A., Murphy, P.M. and Farber, J.M. (1999) *CHEMOKINE RECEPTORS AS HIV-1 CORECEPTORS: Roles in Viral Entry, Tropism, and Disease*, *Annu. Rev. Immunol*. Available at: www.annualreviews.org.

Bester, S.M. *et al.* (2020) "Structural and mechanistic bases for a potent HIV-1 capsid inhibitor," *Science*, 370(6514), pp. 360–364. Available at: https://doi.org/10.1126/science.abb4808.

Blackard, J.T., Cohen, D.E. and Mayer, K.H. (2022) *Human Immunodeficiency Virus Superinfection and Recombination: Current State of Knowledge and Potential Clinical Consequences*. Available at: https://academic.oup.com/cid/article/34/8/1108/283664.

Boldescu, V. *et al.* (2017) "Broad-spectrum agents for flaviviral infections: dengue, Zika and beyond," *Nature Reviews Drug Discovery*, 16(8), pp. 565–586. Available at: https://doi.org/10.1038/nrd.2017.33.

Brenner, B.G. *et al.* (2023) "Doravirine responses to HIV-1 viruses bearing mutations to NRTIs and NNRTIs under *in vitro* selective drug pressure," *Journal of Antimicrobial Chemotherapy*, 78(8), pp. 1921–1928. Available at: https://doi.org/10.1093/jac/dkad184.

Buonaguro, L., Tornesello, M.L. and Buonaguro, F.M. (2007) "Human Immunodeficiency Virus Type 1 Subtype Distribution in the Worldwide Epidemic: Pathogenetic and Therapeutic

Implications," *Journal of Virology*, 81(19), pp. 10209–10219. Available at: https://doi.org/10.1128/jvi.00872-07.

Catania, J.A. *et al.* (1995) *Risk Factors for HIV and Other Sexually Transmitted Diseases and Prevention Practices among US Heterosexual Adults: Changes from 1990 to 1992*.

Chen, J. *et al.* (2022a) "The reservoir of latent HIV," *Frontiers in Cellular and Infection Microbiology*. Frontiers Media S.A. Available at: https://doi.org/10.3389/fcimb.2022.945956.

Chen, J. *et al.* (2022b) "The reservoir of latent HIV," *Frontiers in Cellular and Infection Microbiology*. Frontiers Media S.A. Available at: https://doi.org/10.3389/fcimb.2022.945956.

Clavel, F. *et al.* (1986) "Isolation of a New Human Retrovirus from West African Patients with AIDS," *Science*, 233(4761), pp. 343–346. Available at: https://doi.org/10.1126/science.2425430.

Coffin, J.M. (1995) "HIV Population Dynamics in Vivo: Implications for Genetic Variation, Pathogenesis, and Therapy."

Dando, T.M. and Perry, C.M. (2003) *Enfuvirtide*, *Drugs*.

Deigendesch, N. and Stenzel, W. (2018) "Acute and chronic viral infections," *Handbook of Clinical Neurology*, 145, pp. 227–243. Available at: https://doi.org/10.1016/B978-0-12-802395-2.00017-1.

Doms, R.W. and Peiper, S.C. (1997) *MINIREVIEW Unwelcomed Guests with Master Keys: How HIV Uses Chemokine Receptors for Cellular Entry*, *VIROLOGY*.

Dvory-Sobol, H. *et al.* (2022) "Lenacapavir: A first-in-class HIV-1 capsid inhibitor," *Current Opinion in HIV and AIDS*. Lippincott Williams and Wilkins, pp. 15–21. Available at: https://doi.org/10.1097/COH.0000000000000713.

Fact sheets - UNAIDS (2025).

Freed, E.O. (2002) *HIV-1 Replication*.

Gallo, R.C. *et al.* (1983) "Isolation of Human T-Cell Leukemia Virus in Acquired Immune Deficiency Syndrome (AIDS)."

Gallo, R.C. *et al.* (1984) "Frequent Detection and Isolation of Cytopathic Retroviruses (HTLV-III) from Patients with AIDS and at Risk for AIDS."

Gama-Norton, L. *et al.* (2011) "Lentivirus production is influenced by sv40 large t-antigen and chromosomal integration of the vector in hek293 cells," *Human Gene Therapy*, 22(10), pp. 1269–1279. Available at: https://doi.org/10.1089/hum.2010.143.

García-Serradilla, M., Risco, C. and Pacheco, B. (2019) "Drug repurposing for new, efficient, broad spectrum antivirals," *Virus Research*, 264, pp. 22–31. Available at: https://doi.org/10.1016/J.VIRUSRES.2019.02.011.

Guttman, M. *et al.* (2012) “Solution Structure, Conformational Dynamics, and CD4-Induced Activation in Full-Length, Glycosylated, Monomeric HIV gp120,” *Journal of Virology*, 86(16), pp. 8750–8764. Available at: https://doi.org/10.1128/jvi.07224-11.

Guyader, M. *et al.* (1987) *Genome organization and transactivation of the human immunodeficiency virus type 2*.

Hitchcock, A.M. *et al.* (2024) “Lenacapavir: A novel injectable HIV-1 capsid inhibitor,” *International Journal of Antimicrobial Agents*, 63(1), p. 107009. Available at: https://doi.org/10.1016/J.IJANTIMICAG.2023.107009.

HIV and AIDS: The Basics; HIV.gov (2025). Available at: https://hivinfo.nih.gov/understanding-hiv/fact-sheets/hiv-and-aids-basics#:~:text=The.

HIV and Opportunistic Infections - HIV.gov (2025). Available at: https://hivinfo.nih.gov/understanding-hiv/fact-sheets/what-opportunistic-infection.

HIV Drug Classes - Fact sheets; HIV.gov (2025). Available at: https://doi.org/https://hivinfo.nih.gov/understanding-hiv/fact-sheets/fda-approved-hiv-medicines?utm_source=chatgpt.com.

HIV information sheet - WHO (2025). Available at: https://doi.org/https://www.who.int/news-room/fact-sheets/detail/hiv-aids.

Kawamoto, A. *et al.* (2008) “2'-Deoxy-4'-C-ethynyl-2-halo-adenosines active against drug-resistant human immunodeficiency virus type 1 variants,” *The International Journal of Biochemistry & Cell Biology*, 40(11), pp. 2410–2420. Available at: https://doi.org/10.1016/J.BIOCEL.2008.04.007.

Kelley, C.F. *et al.* (2025) “Twice-Yearly Lenacapavir for HIV Prevention in Men and Gender-Diverse Persons,” *New England Journal of Medicine*, 392(13), pp. 1261–1276. Available at: https://doi.org/10.1056/nejmoa2411858.

Li, Y., Yin, Y. and Mariuzza, R.A. (2013) “Structural and biophysical insights into the role of CD4 and CD8 in T cell activation,” *Frontiers in Immunology*. Frontiers Media SA. Available at: https://doi.org/10.3389/fimmu.2013.00206.

Link, J.O. *et al.* (2020) “Clinical targeting of HIV capsid protein with a long-acting small molecule,” *Nature*, 584(7822), pp. 614–618. Available at: https://doi.org/10.1038/s41586-020-2443-1.

Margot, N. *et al.* (2021) *Absence of Lenacapavir (GS-6207) Phenotypic Resistance in HIV Gag Cleavage Site Mutants and in Isolates with Resistance to Existing Drug Classes*. Available at: https://doi.org/10.

Margot, N.A. *et al.* (2025) "Resistance Analyses in Heavily Treatment-Experienced People with HIV Treated with the Novel HIV Capsid Inhibitor Lenacapavir after 2 Years," *Journal of Infectious Diseases*, 231(5), pp. 1239–1245. Available at: https://doi.org/10.1093/infdis/jiaf050.

Markham, A. (2018) "Ibalizumab: First Global Approval," *Drugs*, 78(7), pp. 781–785. Available at: https://doi.org/10.1007/s40265-018-0907-5.

Marzolini, C. *et al.* (2025) "Drug-drug interactions potential with the HIV-1 capsid inhibitor lenacapavir," *Expert Opinion on Drug Metabolism and Toxicology*. Taylor and Francis Ltd., pp. 161–172. Available at: https://doi.org/10.1080/17425255.2024.2415295.

Mbondji-Wonje, C. *et al.* (2020) "Genetic variability of the U5 and downstream sequence of major HIV-1 subtypes and circulating recombinant forms," *Scientific Reports*, 10(1). Available at: https://doi.org/10.1038/s41598-020-70083-1.

Milan Bonotto, R. *et al.* (2022) "Virucidal Activity of the Pyridobenzothiazolone Derivative HeE1-17Y against Enveloped RNA Viruses.," *Viruses*, 14(6). Available at: https://doi.org/10.3390/v14061157.

Miller, C.J. *et al.* (2005) "Propagation and Dissemination of Infection after Vaginal Transmission of Simian Immunodeficiency Virus," *Journal of Virology*, 79(17), pp. 11552–11552. Available at: https://doi.org/10.1128/jvi.79.17.11552.2005.

Mohammadi, P. *et al.* (2014) "Dynamics of HIV Latency and Reactivation in a Primary CD4+ T Cell Model," *PLoS Pathogens*, 10(5). Available at: https://doi.org/10.1371/journal.ppat.1004156.

Müller, T.G. *et al.* (2022) "Annual Review of Virology Nuclear Capsid Uncoating and Reverse Transcription of HIV-1," 16, p. 39. Available at: https://doi.org/10.1146/annurev-virology-020922.

Murchu, E.O. *et al.* (2022) "Oral pre-exposure prophylaxis (PrEP) to prevent HIV: A systematic review and meta-analysis of clinical effectiveness, safety, adherence and risk compensation in all populations," *BMJ Open*, 12(5). Available at: https://doi.org/10.1136/bmjopen-2020-048478.

Nachega, J.B. *et al.* (2023) "Long-acting antiretrovirals and HIV treatment adherence.," *The lancet. HIV*, 10(5), pp. e332–e342. Available at: https://doi.org/10.1016/S2352-3018(23)00051-6.

Nair, M. *et al.* (2024) "Global and regional genetic diversity of HIV-1 in 2010–21: systematic review and analysis of prevalence," *The Lancet Microbe*, 5(11). Available at: https://doi.org/10.1016/S2666-5247(24)00151-4.

Neverette, N.C. *et al.* (2025) "Lenacapavir: Playing the Long Game in the New Era of Antiretrovirals," *Clinical Pharmacology and Therapeutics*. John Wiley and Sons Inc, pp. 353–367. Available at: https://doi.org/10.1002/cpt.3447.

Nguyen, D.H. and Hildreth, J.E.K. (2000) *Evidence for Budding of Human Immunodeficiency Virus Type 1 Selectively from Glycolipid-Enriched Membrane Lipid Rafts*, *JOURNAL OF VIROLOGY*. Available at: https://journals.asm.org/journal/jvi.

Nka, A.D. *et al.* (2023) "Evaluation of HIV-1 capsid genetic variability and lenacapavir (GS-6207) drug resistance-associated mutations according to viral clades among drug-naive individuals," *Journal of Antimicrobial Chemotherapy*, 78(1), pp. 272–275. Available at: https://doi.org/10.1093/jac/dkac388.

Nyamweya, S. *et al.* (2013) "Comparing HIV-1 and HIV-2 infection: Lessons for viral immunopathogenesis," *Reviews in Medical Virology*, pp. 221–240. Available at: https://doi.org/10.1002/rmv.1739.

Ogbuagu, O. *et al.* (2025) "Efficacy and Safety of Long-Acting Subcutaneous Lenacapavir in Heavily Treatment-Experienced People with Multidrug-Resistant HIV-1: Week 104 Results of a Phase 2/3 Trial," *Clinical Infectious Diseases*, 80(3), pp. 566–574. Available at: https://doi.org/10.1093/cid/ciae423.

Omoding, D. *et al.* (2025) "Subtypes A1 and D, and recombinant HIV-1 natural polymorphisms associated with lenacapavir drug resistance in Uganda," *Journal of Antimicrobial Chemotherapy*, 80(4), pp. 955–961. Available at: https://doi.org/10.1093/jac/dkaf018.

Peeters, M. *et al.* (1997) "Geographical distribution of HIV-1 group O viruses in Africa."

Perelson, A.S. *et al.* (1996) *HIV-1 Dynamics in Vivo: Virion Clearance Rate, Infected Cell Life-span, and Viral Generation Time*, *J. Gen. Virol*.

Pierson, T.C. and Diamond, M.S. (2020) "The continued threat of emerging flaviviruses.," *Nature microbiology*, 5(6), pp. 796–812. Available at: https://doi.org/10.1038/s41564-020-0714-0.

Plantier, J.C. *et al.* (2009) "A new human immunodeficiency virus derived from gorillas," *Nature Medicine*, 15(8), pp. 871–872. Available at: https://doi.org/10.1038/nm.2016.

Pommier, Y., Johnson, A.A. and Marchand, C. (2005) "Integrase inhibitors to treat HIV/AIDS," *Nature Reviews Drug Discovery*, pp. 236–248. Available at: https://doi.org/10.1038/nrd1660.

Popovic, M. *et al.* (1984) *Detection, Isolation, and Continuous Production of Cytopathic Retroviruses (HTLV-III) from Patients with AIDS and Pre-AIDS*.

Princen, K. *et al.* (2004) *Establishment of a novel CCR5 and CXCR4 expressing CD4 + cell line which is highly sensitive to HIV and suitable for high-throughput evaluation of CCR5 and CXCR4 antagonists*. Available at: http://www.retrovirology.com/content/1/1/2.

Ramdas, P. *et al.* (2020) “From Entry to Egress: Strategic Exploitation of the Cellular Processes by HIV-1,” *Frontiers in Microbiology*. Frontiers Media S.A. Available at: https://doi.org/10.3389/fmicb.2020.559792.

Ripamonti, D., Borghetti, A. and Zazzi, M. (2024) “Appropriateness of virological monitoring with long-acting injectable cabotegravir and rilpivirine,” *Journal of Antimicrobial Chemotherapy*, 79(10), pp. 2720–2724. Available at: https://doi.org/10.1093/jac/dkae257.

Sauter, D. *et al.* (2011) “HIV-1 Group P is unable to antagonize human tetherin by Vpu, Env or Nef.,” *Retrovirology*, 8, p. 103. Available at: https://doi.org/10.1186/1742-4690-8-103.

Sayana, S. and Khanlou, H. (2009) “Maraviroc: A new CCR5 antagonist,” *Expert Review of Anti-Infective Therapy*, 7(1), pp. 9–19. Available at: https://doi.org/10.1586/14787210.7.1.9.

Scarsi, K.K. *et al.* (2020) “HIV-1 Integrase Inhibitors: A Comparative Review of Efficacy and Safety,” *Drugs*. Adis, pp. 1649–1676. Available at: https://doi.org/10.1007/s40265-020-01379-9.

Schröder, A.R.W. *et al.* (2002) “HIV-1 Integration in the Human Genome Favors Active Genes and Local Hotspots,” *Cell*, 110(4), pp. 521–529. Available at: https://doi.org/10.1016/S0092-8674(02)00864-4.

Segal-Maurer, S. *et al.* (2022) “Capsid Inhibition with Lenacapavir in Multidrug-Resistant HIV-1 Infection,” *New England Journal of Medicine*, 386(19), pp. 1793–1803. Available at: https://doi.org/10.1056/nejmoa2115542.

Seval, N., Frank, C. and Kozal, M. (2021) “Fostemsavir for the treatment of HIV,” *Expert Review of Anti-Infective Therapy*, 19(8), pp. 961–966. Available at: https://doi.org/10.1080/14787210.2021.1865801.

Sharma, S.C. *et al.* (2018) “Male circumcision for the prevention of human immunodeficiency virus (HIV) acquisition: a meta-analysis,” *BJU International*. Blackwell Publishing Ltd, pp. 515–526. Available at: https://doi.org/10.1111/bju.14102.

Sharp, P.M. and Hahn, B.H. (2011) “Origins of HIV and the AIDS pandemic,” *Cold Spring Harbor Perspectives in Medicine*, 1(1). Available at: https://doi.org/10.1101/cshperspect.a006841.

Simon, V., Ho, D.D. and Abdool Karim, Q. (2006) “HIV/AIDS epidemiology, pathogenesis, prevention, and treatment,” *Lancet*. Elsevier B.V., pp. 489–504. Available at: https://doi.org/10.1016/S0140-6736(06)69157-5.

Smith, S.J. *et al.* (2021) “Integrase strand transfer inhibitors are effective anti-hiv drugs,” *Viruses*. MDPI AG. Available at: https://doi.org/10.3390/v13020205.

Sunlenca prescription label (no date). Available at: www.fda.gov/medwatch.

Teasdale, C., Marais, B. and Abrams, E. (2011) *HIV: prevention of mother-to-child transmission*.

Turner, B.G. and Summers, M.F. (2001) *Structural Biology of HIV*. Available at: http://www.idealibrary.com.

Turner, D., Brenner, B. and Wainberg, M.A. (2003) "Multiple effects of the M184V resistance mutation in the reverse transcriptase of human immunodeficiency virus type 1.," *Clinical and diagnostic laboratory immunology*, 10(6), pp. 979–81. Available at: https://doi.org/10.1128/cdli.10.6.979-981.2003.

Vanhamel, J., Bruggemans, A. and Debyser, Z. (2019) "Establishment of latent HIV-1 reservoirs: what do we really know?," *Journal of Virus Eradication*, 5(1), pp. 3–9. Available at: https://doi.org/10.1016/S2055-6640(20)30275-2.

Wei, X. *et al.* (2002) "Emergence of resistant human immunodeficiency virus type 1 in patients receiving fusion inhibitor (T-20) monotherapy," *Antimicrobial Agents and Chemotherapy*, 46(6), pp. 1896–1905. Available at: https://doi.org/10.1128/AAC.46.6.1896-1905.2002.

Wensing, A.M.J., van Maarseveen, N.M. and Nijhuis, M. (2010) "Fifteen years of HIV Protease Inhibitors: raising the barrier to resistance," *Antiviral Research*, pp. 59–74. Available at: https://doi.org/10.1016/j.antiviral.2009.10.003.

WHO (2025) *Therapeutics and COVID-19 - living guidelines*. World Health Organization. Available at: https://doi.org/10.2471/B09540.

Wyatt, R. *et al.* (1998) "The antigenic structure of the HIV gp120 envelope glycoprotein."

Zhang, H., Dornadula, G. and Pomerantz, R.J. (1998) *Natural endogenous reverse transcription of HIV-1*, *Journal of Reproductive Immunology*.

Zhang, Z.-Q. *et al.* (2004) *Roles of substrate availability and infection of resting and activated CD4 T cells in transmission and acute simian immunodeficiency virus infection*. Available at: www.pnas.orgcgidoi10.1073pnas.0308425101.

7 PUBLICATIONS